Epigenetic reprogramming of human macrophages by an intestinal pathogen

Indra Bekere[1*], Jiabin Huang[1], Marie Schnapp[1], Maren Rudolph[1], Laura Berneking[1], Klaus Ruckdeschel[1], Adam Grundhoff[2], Thomas Günther[2], Nicole Fischer[1], Martin Aepfelbacher[1*]

[1]Institute of Medical Microbiology, Virology and Hygiene, University Medical Center Hamburg-Eppendorf (UKE), Hamburg, Germany

[2] Heinrich-Pette-Institute (HPI), Leibniz Institute for Experimental Virology, Research Group Virus Genomics, Hamburg, Germany

* Corresponding authors

E-mail: ibekere@uke.de (IB), m.aepfelbacher@uke.de (MAe)

Abstract

Various pathogens systematically reprogram gene expression in innate immune cells, but the underlying mechanisms are largely unknown. We investigated whether the enteropathogen *Yersinia enterocolitica* alters chromatin states to reprogram gene expression in primary human macrophages. Genome-wide chromatin immunoprecipitation (ChIP) seq analyses showed that pathogen-associated molecular patterns (PAMPs) induced up- or down-regulation of histone modifications (HM) at approximately 14500 loci in promoters and enhancers. Effectors of *Y. enterocolitica* reorganized about half of these dynamic HM, with the effector YopP being responsible for about half of these modulatory activities. The reorganized HM were associated with genes involved in immune response and metabolism. Remarkably, the altered HM also associated with 61 % of all 534 known Rho GTPase pathway genes, revealing a new level in Rho GTPase regulation and a new aspect of bacterial pathogenicity. Changes in HM were associated to varying degrees with corresponding gene expression, e. g. depending on chromatin localization and cooperation of the HM. Overall, *Y. enterocolitica* profoundly reorganizes HM in human macrophages to reprogram key gene expression programs of the innate immune response.

Author Summary

Human pathogenic bacteria can affect epigenetic histone modifications to modulate gene expression in host cells. However, a systems biology analysis of this bacterial virulence mechanism in immune cells has not been performed. Here we analyzed genome-wide epigenetic histone modifications and associated gene expression changes in primary human macrophages infected with enteropathogenic *Yersinia enterocolitica*. We demonstrate that *Yersinia* virulence factors extensively reprogram the histone modifications and associated gene expression triggered by the pathogen-associated molecular patterns (PAMPs) of the

bacteria. The epigenetically modulated genes are involved in several key pathways of the macrophage immune response, including the Rho GTPase pathway, revealing a novel level of Rho GTPase regulation by a bacterial pathogen. Overall, our findings provide an in-depth view of epigenetic and gene expression changes during host-pathogen interaction and might have further implications for understanding of the innate immune memory in macrophages.

Introduction

Macrophages play an essential role in the response to bacterial infection. They sense pathogen-associated molecular patterns (PAMPs) like lipopolysaccharide (LPS), nucleic acids or flagellin through Toll-like, RIG-I-like or NOD-like pattern recognition receptors (PRRs), respectively (Zhang & Mosser, 2008; Takeuchi & Akira, 2010). RIG-I-like and NOD-like PRRs are part of inflammasomes that process and release the major pro-inflammatory cytokines interleukin (IL)-1β and IL-18 (Broz & Dixit, 2016; Lupfer et al., 2015). While PRRs recognize a wide variety of PAMPs, their downstream signaling often converges on mitogen activated protein kinase- (MAPK), nuclear factor κB- (NF-κB) and type I interferon (IFN) signal pathways (Mogensen, 2009; Takeuchi & Akira, 2010). These pathways include activation of transcription factors that control expression of genes for cytokines, chemokines, and inflammasome components, as well as genes for metabolism, cytoskeleton regulation, and transcriptional regulation (Takeuchi & Akira, 2010; Christgen et al., 2020; Ryan & O'Neill, 2020; Doyle et al., 2004; Roach et al., 2007). Thousands of functionally diverse genes are up- or downregulated by PAMPs in macrophages. Many of these genes belong to elaborate transcriptional programs that drive macrophage functions during infection. Such programs contribute crucially to the immunological phenomena of priming, tolerance (immunosuppression) and trained immunity (Park et al., 2017; Saeed et al., 2014). The inflammatory gene expression programs in macrophages form an intricate network that is characterized by crosstalk and feedback loops (Park et al., 2017; Kang et al., 2019). Because of their central role in immune defense, numerous pathogenic bacteria have developed mechanisms to suppress or modulate macrophage gene expression (Diacovich & Gorvel, 2010).

Pathogenic *Yersinia* species, which comprise the entero-pathogens *Y. pseudotuberculosis* and *Y. enterocolitica* as well as the plague agent *Yersinia pestis*, proliferate extracellularly in

lymphoid tissues of animal hosts (Balada-Llasat & Mecsas, 2006; Viboud & Bliska, 2005). Therefore, the bacteria suppress phagocytosis, migration and immune signaling in resident cells of the innate immune system (Viboud & Bliska, 2005; Marketon et al., 2005). The major virulence mechanism of pathogenic yersiniae is a type III secretion system (T3SS) by which they inject effector proteins, named *Yersinia* outer proteins (Yops), into immune cells (Cornelis & Wolf-Watz, 1997; Galán & Wolf-Watz 2006; Viboud & Bliska, 2005). The seven known Yops exert different activities to suppress immune cell functions. E.g., YopE, YopT and YopO block cytoskeletal reorganization by modifying the activity of Rho GTP binding proteins (Aktories et al., 2000; Aepfelbacher & Wolters, 2017). Further, YopP/J, and YopM inhibit the inflammatory responses triggered by the PAMPs or the damage associated molecular patterns (DAMPs) elicited by the bacteria (Brodsky et al., 2010; Chung et al., 2016; Mukherjee et al., 2006; Schubert et al., 2020). Production of DAMPs is a consequence of bacterial virulence activities in host cells and DAMPs are also sensed by PRRs. *Yersinia*-induced DAMPs are e.g. produced in response to membrane damage caused by the T3SS translocation pore or by deactivation of Rho GTPases through YopE and YopT (Schubert et al., 2020). YopP/J acetylates and inhibits components of NF-κB and MAPK pathways and thereby profoundly suppresses pro-inflammatory gene expression downstream of TLRs (Mukherjee et al., 2006). YopM acts by both, increasing production of the anti-inflammatory cytokine IL-10 and counteracting activation of the pyrin inflammasome, which is triggered by the Yop-induced deactivation of Rho GTPases (McPhee et al., 2012; Berneking et al., 2016; Chung et al., 2016). Thus, on one hand pathogenic yersiniae contain immunostimulatory PAMPs and their T3SS effectors elicit DAMPs that strongly alter gene expression in macrophages. On the other hand, the bacteria employ an arsenal of activities to systematically modulate and antagonize the PAMP- and DAMP triggered immune responses (Philip et al., 2016; Schubert et al., 2020).

Epigenetic mechanisms play a master role in the regulation of macrophage gene expression. Amongst others they i) determine the phenotypes of macrophages in different tissues and disease states, ii) control trained innate immunity, iii) regulate priming and immune tolerance and iv) integrate stimulus triggered responses (Ivashkiv, 2013; Park et al., 2017; Glass & Natoli, 2015; Saeed et al., 2014). Gene expression in response to external stimuli is controlled by the concerted activity and binding of macrophage lineage-determining transcription factors and stimulus-regulated transcription factors to accessible cis-regulatory elements (promoters and enhancers) in the cellular chromatin (Ivashkiv, 2013; Glass & Natoli, 2015). DNA accessibility is determined by the pre-existing epigenomic landscape, which is the sum of DNA methylation, nucleosome occupancy, pre-bound factors and histone modifications (Klemm et al., 2019). The types of histone modifications located at gene promoters and enhancers determine DNA accessibility and transcriptional activity. For instance, a trimethylated lysine at position 4 in histone 3 (H3K4me3) is characteristic for active promoters, H3K27ac indicates active promoters and enhancers while H3K9me3 signifies repressed, transcriptionally inactive heterochromatin (Rada-Iglesias et al., 2011; Barski et al., 2007; Wang et al., 2008). Most posttranslational histone modifications are transient and their turnover is regulated by enzymes that mediate their deposition or deletion (Yun et al., 2011; Allis & Jenuwein, 2016).

Bacterial PAMP-induced signaling has been shown to intensely modulate histone modifications and this has been implicated in priming, immune tolerance and trained immunity in macrophages (Ivashkiv, 2013; Park et al., 2017; Dong & Hamon, 2020; Saeed et al., 2014). Consequently, numerous pathogens can interfere with histone modifications in host cells using unique and sophisticated strategies (Connor et al., 2019; Bierne et al., 2012; Rolando et al., 2013).

The current understanding of how *Yersinia* modulates gene expression in macrophages is that it uses its effectors YopP and YopM to interfere with PAMP-induced MAP-kinase and NF-kB

signaling to the nucleus (Schubert et al., 2020). Previous systematic studies of *Yersinia* effects on gene expression were conducted with gene arrays and cultured mouse macrophages infected for up to 2.5 h (Sauvonnet et al., 2002; Hoffmann et al., 2004). Here we employed primary human macrophages and genome wide chromatin immunoprecipitation (ChIP)-seq and RNA-seq technologies to globally analyze histone modifications and associated gene expression patterns for up to 6 h of *Y. enterocolitica* infection. We uncover a profound and coordinated reprogramming of histone modifications as basis for *Yersinia's* systematic effect on gene expression. In addition to extensively modulating HM at inflammatory, immune response and metabolism genes, the bacteria altered HM at 61 % of all 534 known Rho GTPase pathway genes in macrophages.

These results describe the previously unrecognized strategy of pathogenic *Yersinia* to modulate specific gene expression programs in innate immune cells through the systematic reorganization of histone modifications.

Results

Global reprogramming of histone modifications in macrophages by *Yersinia enterocolitica*

We first investigated on a global scale whether *Y. enterocolitica* alters histone modification patterns in human macrophages (Ivashkiv, 2013). For this, *in vitro* differentiated primary human macrophages were mock infected or infected with *Y. enterocolitica* wild type strain WA314 or its avirulent derivative WAC and subjected to chromatin immunoprecipitation (ChIP)-seq (Fig 1A). WAC lacks a T3SS and therefore was used to separate the effects of the *Yersinia* PAMPs from the T3SS associated effects (S1 Table). We investigated cells at 6 h after infection, a time point at which a maximal effect on gene expression but no signs of apoptosis are detectable in the human macrophages (Berneking et al., 2016; Ruckdeschel et al., 1997; Sarhan et al., 2018). Analyzes were performed for four histone-3 (H3) marks whose impact on macrophage gene expression has been well established: H3K4me3, indicating active promoters; H3K4me1, which is highly enriched at distal regulatory elements (enhancers) but is also found with lower levels at promoters; H3K27ac, indicating active promoters and enhancers; and H3K27me3 indicating inactive promoters and enhancers (Heintzman et al., 2009; Rada-Iglesias et al., 2011; Barski et al., 2007; Wang et al., 2008). Dynamic regions were defined as those exhibiting at least a 2-fold change in any pairwise comparison between mock-, WA314- or WAC infected macrophages. Overall, H3K27ac peaks were the most dynamic (43 %) followed by H3K4me3 peaks (7 %), H3K4me1 regions (3 %) and H3K27me3 regions (0.1 %) (Fig 1B, S1A Fig). Around half of the dynamic H3K4me3 peaks and H3K4me1 regions and one fourth of the dynamic H3K27ac peaks were at promoters (+/- 2 kb from transcription start site; Fig 1C and S1A Fig). The remaining half of the dynamic H3K4me3 peaks and H3K4me1 regions and three fourth of the dynamic

H3K27ac peaks were at enhancers (H3K4me1-enriched regions outside promoters; Fig 1C and S1A Fig).

A Spearman correlation heatmap of the H3K27ac peaks and two corresponding datasets published elsewhere from naive and *E. coli* LPS-stimulated primary human macrophages (Park et al., 2017; Novakovic et al., 2016) revealed i) a strong correlation between WAC infected and LPS-treated macrophages, indicating that the PAMP-induced histone modifications are to a large part caused by LPS, although yersiniae possess a number of additional PAMPs (Fig 1D) (Reinés et al., 2012; Zhou et al., 2018; Brodsky et al., 2010); ii) a close similarity between the mock-infected macrophages in our study and the naïve macrophages employed in other studies, and iii) a higher similarity of WA314 infected macrophages to naïve and mock-infected macrophages than to WAC- and LPS infected macrophages (Fig 1D). This likely reflects suppression of PAMP/LPS-induced H3K27ac modifications by the T3SS effectors of WA314 (Schubert et al., 2020).

We evaluated whether histone marks were significantly ($\geq$ 2-fold change, adjusted P-value $\leq$ 0.05) up- or down-regulated in the three pairwise comparisons WAC vs mock, WA314 vs mock and WAC vs WA314 (Fig 1E). An eminent result was that, consistently, around 14-times more H3K27ac regions than H3K4me3 regions were dynamic and roughly similar numbers of H3K27ac marks were up- and down regulated in each comparison (Fig 1E). At the same time, there was H3K4me3 upregulation at a considerable number of loci (280 to 1081), whereas only a minor number of loci (44 to 173) exhibited H3K4me3 down regulation in the three comparison groups (Fig 1E). Further, 2156 unique H3K4me1 regions were dynamic with roughly similar numbers up- and down regulated (Fig 1E). H3K27me3 regions were essentially unaltered under these conditions, further suggesting that H3K27me3 marks are not affected by *Yersinia* infection in macrophages (S1B Fig). WAC up- and down-regulated histone modifications at 14559 unique loci with vs mock, reflecting the effect of the pathogen-associated molecular patterns (PAMPs). Overall, WAC and WA314 up- or down

regulated histone marks at promoters and enhancers of 7745 and 5900 genes, respectively (S1C Fig). As determined by comparison with the WAC effects, WA314 inhibited the up regulation of 571 H3K4me3 regions (53 %; Fig 1F) and 2881 H3K27ac regions (42 %; Fig 1G) and inhibited the down regulation of 2627 H3K27ac regions (40 %; Fig 1G).

Further analyses revealed that the *Yersinia* altogether remodeled histone modification patterns at 10994 unique genes (Fig 1H). Patterns were modified at promoters of 6228 genes and at enhancers of 7730 genes (Fig 1H). Thereby, 2964 genes were modified both at the promoter and nearby enhancer regions (Fig 1H).

We conclude that *Y. enterocolitica* extensively reprograms chromatin states in human macrophages by regulating H3K27ac-, H3K4me1- and H3K4me3 marks at promoters and enhancers of about 11000 genes (Fig 1H).

Y. enterocolitica alters histone modifications at promoters

We investigated the bacteria induced reprogramming of histone modifications at promoters in more detail. By genome wide analysis of dynamic H3K27ac and H3K4me3 regions at promoters of mock-, WAC- and WA314 infected macrophages we identified 10 clusters which could be assigned to 6 classes and 2 modules (Methods; Fig 2A, S2 Table). Promoter module 1 (P1) contains dynamic H3K4me3- and H3K27ac regions that change concordantly (classes P1a, b; Figs 2A, B). Promoter module 2 (P2) contains dynamic H3K27ac regions at largely constant H3K4me3 regions (classes P2a-d; Figs 2A, B). The patterns of histone modifications in the classes were clearly distinct and assigned to 4 different profiles. In profile “Suppression”, WAC increases deposition of histone marks and this is suppressed by WA314 (P1a and P2a; Figs 2A-C). In profile “Prevention”, WAC downregulates histone marks and this is prevented by WA314 (P1b and P2d; Figs 2A-C). In profile “Down”, WA314 selectively downregulates H3K27ac marks when compared to mock and WAC (P2b;

Figs 2A, B, D). In profile "Up" WA314 selectively upregulates H3K27ac marks when compared to mock and WAC (P2c; Figs 2A, B, D). These profiles are also illustrated by tag densities of H3K4me3 and H3K27ac ChIP-seq at promoters of selected genes (Figs 2C, D). Although WA314 strongly counteracted the PAMP-induced up- and downregulation of histone modifications at promoters, the counter-regulation often was not complete. Therefore, the levels of histone modifications in WA314 infected cells were frequently in between the levels in mock- and WAC infected macrophages (e.g. in Suppression profile classes P1a and P2a; Figs 2A, B).

In summary, four profiles describe how *Y. enterocolitica* alters H3K4me3 and H3K27ac marks at macrophage promoters. In the profiles Suppression and Prevention the bacteria's T3SS effectors block the PAMP-induced deposition or removal of H3K4me3- and H3K27ac marks, respectively (Fig 2E). In profiles Down and Up the T3SS-associated effectors down- or up-regulate, respectively, H3K27ac marks.

Reprogramming of enhancer associated histone modifications by *Y. enterocolitica*

We sought to investigate in detail the *Yersinia* induced reprogramming of histone modifications at distal regulatory elements/enhancers. A genome wide heatmap of dynamic H3K27ac regions at enhancer regions, characterized by the presence of H3K4me1 marks, was prepared in mock-, WAC- and WA314 infected macrophages (Fig 3A, S3 Table). Six clusters comprising altogether 16408 dynamic enhancers were identified and assembled into four classes (E1-E4; Fig 3A). Analogous to the promoter classes, the enhancer classes E1, E2, E3 and E4 correspond to Suppression, Down, Up and Prevention profiles, respectively (Fig 3B). In unstimulated macrophages (mock) enhancers were either poised (no or low level of

H3K27ac marks; E1 and E3) or constitutive (presence of H3K27ac marks; E2 and E4) (Figs 3A, B; Ostuni et al., 2010). WAC infection activated poised enhancers by increasing H3K27ac marks (E1; Fig 3C purple box) or repressed constitutive enhancers by decreasing H3K27ac marks (E4) (Figs 3A, B). WA314 inhibited the WAC induced up-regulation of poised enhancers in Suppression profile E1 and down-regulation of constitutive enhancers in Prevention profile E4 (Figs 3A-C). WA314 also down-regulated constitutive enhancers in Down profile E2 and up-regulated poised enhancers in Up profile E3 (Figs 3A, B). We also investigated the effect of *Yersinia* on latent enhancers, defined by the initial absence of H3K4me1- and H3K27ac marks (Ostuni et al., 2010). We identified 149 latent enhancers in mock infected macrophages that gained H3K4me1- and H3K27ac marks upon WAC infection, which converts these latent enhancers into a constitutive state (Fig 3D, S4 Table). WA314 also increased H3K4me1 levels but did not produce an increase of H3K27ac levels in most of these latent enhancers (Fig 3D). Thus, WA314 infection does not inhibit the unveiling of latent enhancers and their conversion into a poised state by the bacterial PAMPs, but suppresses their transition to a constitutive state (Fig 3D).

Taken together, *Y. enterocolitica* remodels H3K4me1- and H3K27ac patterns at poised, constitutive or latent distal regulatory elements/enhancers in macrophages giving rise to Suppression-, Up-, Down- und Prevention profiles.

Changes in gene expression associated with reprogrammed histone modifications at macrophage promoters and enhancers

We asked to what extent the histone modifications reprogrammed by the bacteria affect expression of the corresponding genes. Therefore, infected macrophages were analyzed by RNA-seq in parallel to ChIP-seq (Fig 1A). 6148 differentially expressed genes (DEGs) were altogether found in three pairwise comparisons (WAC vs mock, WA314 vs mock and WAC

vs WA314; Fig 4A; S5 and S6 Tables). Four classes (R1-R4) were identified in the DEGs which corresponded to Suppression- (R1), Down- (R2), Up- (R3) or Prevention (R4) profiles (Fig 4A and S6 Table). WAC up-regulated 3020 genes (Fig 4B) and down-regulated 2152 genes (Fig 4C) vs mock reflecting the transcriptional response of macrophages to the PAMPs of *Y. enterocolitica.* In the Suppression profile, 42 % of the genes upregulated by WAC were not or only partly upregulated by WA314 (Fig 4B). In the Prevention profile, 39 % of the genes downregulated by WAC were not or much less downregulated by WA314 (Fig 4C). WA314 often did not completely reverse the PAMP-induced up- or downregulation of genes, as shown by the fact that gene expression levels in the WA314 infected cells were frequently in between mock- and WAC infected macrophages (e.g. in classes R1 and R4, Fig 4A). Thus, coinciding with histone modifications, gene expression is modulated extensively by *Y. enterocolitica* in human macrophages and can also be divided into Suppression-, Down-, Up-, and Prevention profiles.

We specifically assessed how histone modifications at promoters affect gene expression and found that 59-73 % of the up-regulated H3K4me3 marks (Fig 4D) and 23-46 % of the up-regulated H3K27ac marks (Fig 4E) showed enhanced expression of the associated genes. When both marks were upregulated 65-81 % of the associated genes showed increased expression (Fig 4F). In comparison, when H3K4me3- and H3K27ac marks were down-regulated individually or in combination, only 8-33 % of the associated genes showed reduced expression (Figs 4D-F). We conclude that while up-regulation of stimulatory histone marks at promoters plays an important role in driving gene expression, downregulation of these marks is less relevant for decreasing gene expression in *Y. enterocolitica* infected macrophages.

In comparison, 5-29 % of the genes associated with H3K27ac marks at enhancers showed changes in gene expression, indicating that enhancer modifications control direct gene expression to a lesser extent than promoter modifications (Fig 4G).

We also evaluated all individual histone modifications which associated with gene expression changes in the different profiles and found that Suppression-, Down-, Up- and Prevention profiles showed on average 30 %, 2 %, 4 % and 16 % corresponding gene expression changes, respectively (Fig 4H).

To find out whether histone modifications at promoters and enhancers cooperate to regulate gene expression, we analyzed pairwise overlaps of genes associated with promoter- and enhancer classes. The strongest overlaps occurred in classes belonging to the same profiles: P1a/P2a/E1 (Suppression), P2b/E2 (Down), P2c/E3 (Up) and P1b/P2d/E4 (Prevention) (Fig 4I). We found that 57 % of the genes overlapping in the Suppression profile classes and 26 % of the genes overlapping in the Prevention profile classes showed corresponding changes in gene expression (S2 Fig). In comparison, only 4 % and 3 % of genes associated with histone modifications in the Down and Up profile classes, respectively, showed expression changes (S2 Fig).

We conclude that reprogramming of histone modifications by *Y. enterocolitica* in macrophages can cause significant changes in gene expression. The size of the effect displays a very wide range from 2 to over 80% and strongly depends on the localization (promoter or enhancers, direction (up or down), cooperation (e.g. at promoters or between related promoters and enhancers) and profile of the histone modifications. A schematic depicts the changes in HM at promoters and enhancers and transcription for selected Suppression and Prevention profile genes (Fig 4J).

Gene pathways associated with alteration of histone modifications by *Y. enterocolitica*

To address the question which biological pathways are regulated by the *Yersinia*-induced epigenetic reprogramming, we subjected all DEGs in the different expression classes/profiles that are associated with histone modifications (Fig 5A) to Gene Ontology (GO) and KEGG analysis (Fig 5B). In profiles Suppression, Down, Up and Prevention, 51 %, 19 %, 19 % and 36 % of genes, respectively, were associated with at least one corresponding histone modification change (Fig 5A). Thus, the proportion of gene expression changes that is associated with histone modifications is clearly higher than the proportion of histone modifications that is associated with corresponding gene expression changes (compare Fig 4H and Fig 5A). Suppression profile genes were most highly enriched in inflammatory response, type I interferon signaling and apoptotic process (Fig 5B) and mainly encode pro-inflammatory cytokines, chemokines, feedback regulators (like TNFAIPs) and type I IFN signaling mediators (Fig 5C, S3A Fig). Down profile was enriched in regulation of transcription (Fig 5B) containing CEBPE and FOS (Fig 5D). CEBPE regulates myeloid lineage commitment and differentiation (Bedi et al., 2009), inflammasome activation and interferon signaling (Göös et al., 2019). FOS encoding c-Fos protein is a part of AP1 complex, which regulates macrophage differentiation and long range enhancer interactions (Phanstiel et al., 2017), suppresses pro-inflammatory cytokine and IL-10 expression and increases lysosome mediated bacterial killing (Hop et al., 2018). Up profile genes were enriched in Wnt signaling (Figs 5B, D), which directs macrophage differentiation, regulates expression of key anti-inflammatory mediators, such as IL-10 and TGF-β, and modulates phagocytosis (Malsin et al., 2019). Prevention profile genes were enriched in pathways involving regulation of GTPases, including mostly Rho GTPase pathway genes (Figs 5B, E) and in metabolic pathways (Fig 5B), including 22 genes for the metabolism of cholesterol, fatty acids, acyl-CoA or glucose (S7 Table). Suppression profile genes associated with latent enhancers (Fig 3D) were enriched among others in negative regulation of transcription and inflammatory signaling (S3B Fig).

Analysis of transcription factor motif enrichment revealed binding sites of inflammatory regulators from the RHD- (NFkB-p65-Rel), IRF- (ISRE, IRF2) and bZIP- (Fra2, Fosl2, Jun-AP1) families in Suppression profile genes (Fig 5F, S5C Fig). No transcription factor motifs were enriched in Down profile. Up profile was enriched for RHD (NFkB-p65-Rel) binding sites (Fig 5F, S5C Fig) indicating that *Yersinia* effector activities can lead to increased gene expression also through regulation of NF-□B signaling. Prevention profile genes were enriched for distinct motifs from ETS (SpiB, PU.1) family (Fig 5F, S5C Fig). ETS TFs are known to interact extensively with other TFs (Verger & Duterque-Coquillaud, 2002) and play a role in cytokine gene expression (Gao et al., 2016; Lennard Richard et al., 2014; O'Reilly et al., 2003; Gallant & Gilkeson, 2006). PU.1 is a lineage determining TF in macrophages which establishes enhancer and promoter landscapes and modulates gene expression (Glass & Natoli, 2015).

Taken together, the histone modifications that *Y. enterocolitica* reprograms control central transcriptional programs in macrophages. Most significantly, PAMP-induced up-regulation of immune signaling and inflammatory response genes is suppressed and the down-regulation of metabolic and Rho GTPase pathway genes is prevented by the bacteria.

Epigenetic reprogramming of Rho GTPase pathway genes by *Y. enterocolitica*

Interestingly, the Rho GTPase pathway was most significantly enriched in Prevention profile genes connected to histone modifications (Figs 5B, E). It was also found enriched in the Suppression profile and in the latent enhancer associated genes (S8 Table). Altogether, the dynamic histone modifications identified here were associated with 324 unique Rho GTPase pathway genes (61 % of all known Rho GTPase genes; Fig 6A, S9 Table).

A great variety of bacterial virulence factors target or imitate Rho proteins or their regulators to manipulate immune cell functions (Heasman & Ridley, 2008; Aktories, 2011). Subversion of Rho-GTPase activities is also a central virulence strategy of *Yersinia* and there is mediated by the T3SS effectors YopE, YopT and YopO/YpkA (Aepfelbacher & Wolters, 2017). However, only scarce information is available on the epigenetic regulation of Rho GTPase pathway genes in general and relevant systems-level studies are lacking (Chen et al., 2020). Considering the strong association of dynamic histone modifications with Rho GTPase pathway genes in *Yersinia* infected macrophages, we examined this connection in more detail here.

The Rho GTPase family is composed of 20 proteins, which can be divided into 8 subfamilies (Boureux et al., 2006). Rho GTPases are best known for regulating the actin cytoskeleton but also control vesicle transport, microtubule dynamics, cell cycle and gene expression (Jaffe & Hall, 2005; Hodge & Ridley, 2016). Through these basic activities, they play central roles in immune cell functions such as phagocytosis, chemotaxis and adhesion (Heasman & Ridley, 2008). The classical Rho GTPases cycle between inactive GDP-bound and active GTP-bound states. Guanine nucleotide exchange factors (GEFs) promote the dissociation of GDP leading to GTP loading and activation (Laurin & Côté, 2014). Active GTP-bound Rho proteins stimulate effector proteins which carry out basic molecular activities (Bagci et al., 2020; Mott

& Owen, 2015). GTPase activating proteins (GAPs) bind to GTP-loaded Rho proteins and thereby stimulate their intrinsic GTPase activity and lead to their deactivation (Tcherkezian & Lamarche-Vane, 2007). Most GEFs, GAPs and effectors are not specific for individual Rho GTPases but associate with members of one or more subfamilies (Müller et al., 2020; Bagci et al., 2020). Currently 77 RhoGEFs (Laurin & Côté, 2014), 66 Rho GAPs (Tcherkezian & Lamarche-Vane, 2007) and up to 370 Rho GTPase effectors are known, whereby the number of effectors may still be growing (Bustelo et al., 2007; Paul et al., 2017; Bagci et al., 2020). Notably, 68 %, 62 %, 58 % and 74 % of all known genes for GAPs, GEFs, effectors and Rho proteins, respectively, exhibited altered histone modification patterns in *Y. enterocolitica* infected macrophages (S4A Fig "RNA & ChIP" and "ChIP only" fractions). Histone modifications were concomitantly altered at enhancers and promoters of 127 Rho GTPase pathway genes (S4B Fig). More than 2 enhancer regions in the E1 and E4 enhancer classes were on average associated with an individual Rho GTPase pathway gene (Fig 6A) and the number of enhancers per Rho GTPase gene ranged from 1 to 14 (S4C Fig, S9 Table). FNBP1, RAPGEF1 and ELMO1 were the genes for which 13, 13 and 14 putative enhancers, respectively, were found (S9 Table).

To draw the most informed conclusion about the biological significance of Rho GTPase pathway gene regulation by *Yersinia*, we created a heatmap of all Rho GTPase pathway DEGs in mock-, WAC-, and WA314-infected macrophages independent of their association with histone modifications (Bustelo et al., 2007; Paul et al., 2017; Bagci et al., 2020; Müller et al., 2020; Wennerberg et al., 2004; Senoo et al., 2019). This revealed altogether 204 DEGs in Suppression-, Down-, Up- and Prevention profiles (classes R1-R4, Fig 6B, S10 Table). Of these, 29 encode GTPase activating proteins (GAPs), 31 guanine nucleotide exchange factors (GEFs), 134 effectors and 11 Rho GTPases (S10 Table). 115 (56 %) of these DEGs were in fact associated with dynamic histone modifications (Fig 6C).

Recently all known proteins with putative GAP or GEF activities were biochemically characterized regarding their actual effect on the three main Rho family proteins RhoA, Rac1 and Cdc42 (Müller et al., 2020). Analysis of our data in view of this report revealed that in the Prevention profile 60 % of the actually active GAPs (6/10) act specifically on Rac as compared to 36 % (18/50) of all known GAPs (Figs 6D, E, S11 Table; Müller et al., 2020). In the Suppression profile, Rho-, Rac- or Cdc42 specific GAP genes are not enriched and the percentages of GAP activities acting on Rho (25 %) or Rac (25 %) are identical to those of total GAPs (Figs 6D, E; Müller et al., 2020). We conclude that aided by epigenetic remodelling *Y. enterocolitica* tends to keep Rac-inhibiting GAPs at the level of uninfected cells.

Of the 8 Rho GTPase genes in the Suppression and Prevention profiles, three encode classical Rho proteins (Rac1, RhoC, RhoG) and five encode atypical Rho proteins (RhoH, RhoU, RND1, RhoBTB1, RhoBTB2) (Fig 6F). Most atypical Rho proteins are considered constitutively active and consequently are not regulated by GEFs and GAPs but instead are controlled at the level of transcription and targeted destruction, i.e. proteasomal degradation (Aspenström et al., 2007; Haga & Ridley, 2016). The cellular levels of RhoC and RhoG were also shown to be transcriptionally regulated (Vincent et al., 1992; Fritz et al., 1999). Classical and atypical Rho proteins often have overlapping cellular functions and share the same effector proteins. Atypical Rho proteins have so far been implicated in multiple activities including tumour suppression (e.g. RhoBTB2), cell transformation and -morphogenesis as well as development (e.g. RhoU and Rnd) (Aspenström et al., 2007; Stiegler & Boggon, 2020; Hodge & Ridley, 2016; Chardin, 2006). Many atypical Rho proteins have been found to regulate the activity of classical Rho Proteins, e.g. RhoH spatially controls Rac1 activity (Tajadura-Ortega et al., 2018) and Rnd proteins bind and steer Rho GAP proteins to specific cell sites (Stiegler & Boggon, 2020). Notably, the Rho protein genes in the Suppression profile include Rac1, the Rac1 activator RhoG and the atypical Rho proteins RhoH and RhoU

(Fig 6F). These Rho proteins can alternatively activate Rac effectors, spatiotemporally control Rac activity or take over Rac functions in cells (Bagci et al., 2020; Aspenström et al., 2007; Hodge & Ridley, 2016; Tajadura-Ortega et al.,2018; Chardin, 2006). Thus, a prominent effect of *Yersinia* in the Suppression profile is to inhibit the expression of genes, whose products can keep up Rac activity. This effect complements well the blocked downregulation of Rac GAPs in the Prevention profile (Figs 6D, E).

Altogether epigenetically controlled gene expression causes low Rac activity in *Yersinia* infected cells and thereby cooperates with the Rac down-regulating T3SS effectors YopE, YopO and YopT (Aepfelbacher & Wolters, 2017).

66 Rho GTPase effectors were altogether found in the overlaps of gene expression and epigenetic profiles (S4A, D, F Figs; Bustelo et al., 2007; Paul et al., 2017; Bagci et al., 2020). This includes effectors for all eight Rho GTPase subfamilies (Rho, Rac, Cdc42, RhoD/Rif, Rnd, Wrch-1/Chp, RhoH and RhoBTB) (S4F Fig, S12 Table). Interestingly, while *Yersinia* prevents downregulation of genes for the atypical RhoBTBs (Fig 6F), it at the same time suppresses expression of genes encoding specific RhoBTB effectors (S4F Fig, S12 Table). Furthermore, 19 of the identified Rho GTPase effectors have been implicated in epigenetic and transcriptional regulation, suggesting mechanisms for crosstalk and feedback in the epigenetic control of Rho GTPase pathway gene expression (S12 Table). Another level of regulation is provided by the finding that some DEGs from Suppression- and Prevention profile genes belong to the machinery for ubiquitination and/or proteasomal degradation of Rho proteins (Fig 6G; Hodge & Ridley, 2016).

Altogether these data indicate that yersiniae modulate expression of a large part of Rho GTPase pathway genes in macrophages through reprogramming cellular chromatin on multiple levels (S4D, E Figs, Figs 6E, F, H).

Role of YopP in epigenetic reprogramming by *Y. enterocolitica*

The *Y. enterocolitica* T3SS effectors YopP (YopJ in *Y. pseudotuberculosis*) and YopM have been shown to modulate inflammatory gene expression in *Yersinia* infected macrophages (Schubert et al., 2020). We therefore examined whether YopP and YopM contribute to the epigenetic reprogramming by *Y. enterocolitica*. Macrophages were infected (6 h) with WA314 strains lacking YopP or YopM (strains WA314ΔYopP or WA314ΔYopM; S1 Table) and investigated using ChIP-seq and RNA-seq (H3K4me3 and H3K27ac modifications; Fig 1A). Principal component analysis (PCA) revealed that the WA314ΔYopM- and WA314 induced H3K27ac- and H3K4me3 modifications located close to each other, while the WA314ΔYopP induced modifications were clearly separate (Fig 7A, S5A Fig). This suggests that YopP but not YopM significantly contributes to the epigenetic changes produced by WA314. The effects of WA314ΔYopP and WA314ΔYopM were directly compared with the effects of WA314 on H3K27ac- and H3K4me3 modifications and gene expression. Notably, 684 H3K4me3 regions and 5094 H3K27ac regions were differentially regulated between WA314ΔYopP and WA314 (Fig 7B). In contrast, altogether only 31 histone modifications were differentially regulated between WA314ΔYopM and WA314 (Fig 7B). While 1616 DEGs were detected between WA314ΔYopP and WA314, also 804 DEGs were found between WA314ΔYopM and WA314 (Fig 7B). This suggests that YopP affects gene transcription in macrophages to a large extent through modulation of H3K27ac- and H3K4me3 histone modifications. In contrast, although YopM strongly affects gene transcription, it does not do so by regulating H3K4me3- and H3K27ac histone modifications. We next studied what proportions of the WA314-induced histone modifications in the Suppression-, Prevention-, and Up- and Down profiles were due to YopP (S5B Fig). For this, the percentage YopP effect was calculated from the ratio of fold change (FC) between WA314ΔYopP vs WA314 and either WA314 vs WAC (Suppression and Prevention profiles) or WA314 vs mock (Up and Down profiles). In the promoter and enhancer classes the median

Yop contribution to the WA314 effects was 42 % and ranged from 8.9 % - 57.2 % (S5B Fig). Furthermore, the median YopP contribution to the WA314 effects on gene expression associated with histone modifications was 51.4 % (S5C Fig). We conclude that YopP on average contributes around one half to the effects of *Y. enterocolitica* on histone modifications and gene expression. Consequently, other T3SS associated virulence factors - except YopM – also contribute significantly.

We looked in more detail at the effects of YopP on Rho GTPase pathway genes (Fig 6, S13 Table). In the Suppression- and Prevention profiles of Rho GTPase pathway genes, YopP contributed in the mean 48.5 % and 78.5 %, respectively, to the WA314 effects (S13 Table). However, at the level of individual genes the YopP effect was widely spread from 2 to 103 % in the Suppression- and from 29 to 177 % in Prevention profile (Fig 7C, S13 Table). We tested whether this widely distributed effect of YopP also applies to inflammatory genes (Fig 5B, S3A Fig, S14 Table). Notably, while the mean effect of YopP on the Suppression profile inflammatory genes was 46 % (S14 Table), the effect on individual genes was spread from -57 to 103 % (Fig 7D). Although the majority of YopP induced changes in gene expression were associated with corresponding YopP induced changes in histone modifications, some YopP regulated genes were associated with histone modifications induced by other T3SS effectors and vice versa (e.g. IL2RA highlighted in Figs 7D, E; S13 and S14 Tables, S5D Fig). Further, although YopP contribution to gene expression and histone modifications was evident for the majority of genes and regions associated with inflammatory response and Rho GTPase pathways, the YopP effects on gene expression on one hand and histone modifications on the other hand frequently did not correlate (S5D Fig). Thus, the YopP effect on the expression of individual Rho GTPase pathway and inflammatory genes varies considerably from representing the complete *Yersinia* wild type effect to just a minor contribution. It thereby appears that different T3SS effectors and histone modifications contribute to the widely varying YopP effects on gene expression.

YopP/YopJ blocks PAMP-induced inflammatory gene expression by inhibiting NF-κB and MAP-kinase signaling (Schubert et al., 2020). Interestingly, MAP-kinases also phosphorylate histone-3 at serine-10, a modification that is thought to promote the deposition of activating histone marks like H3K14ac and H3K16ac (Sawicka & Seiser, 2014). We therefore sought to find out whether YopP reduces the deposition of H3K4me3- and/or H3K27ac marks through inhibition of MAP-kinases. WA314 inhibited the deposition of H3K4me3 at the IDO1- and SOCS3 promoters and deposition of H3K27ac at the SOCS3 and PTGS2 promoters in the macrophages (Fig 7F). YopP contributed to the WA314 effects on these genes, as seen by significantly less inhibitory activity of WA314ΔYopP on deposition of the histone marks when compared to WA314 (Fig 7F). When combined with the MAP-kinase inhibitors SB203580 and PD98059, targeting p38 and MEK1, respectively, WA314ΔYopP was nearly as effective as WA314 in inhibiting the deposition of H3K4me3 marks at the IDO1 and SOCS3 promoters and deposition of H3K27ac marks at the PTGS2 and SOCS3 promoters (Fig 7F). Thus, MAP-kinase inhibitors can substitute for the missing YopP activity in WA314ΔYopP. This is consistent with the idea that YopP blocks deposition of the histone marks through MAP-kinase inhibition.

Finally, we wanted to determine whether the histone modification-driven reprogramming of Rho GTPase pathway genes has functional consequences in macrophages. For this, we took advantage of suppression of ABI1 gene expression by WA314, which is entirely dependent on YopP (Fig 7C and S5D Fig). ABI1 encodes a component of the WAVE regulatory complex that controls actin polymerization in macrophages (Chen et al., 2014; Stahnke et al., 2021). Corresponding to gene expression, the ABI1 protein was upregulated in WA314□YopP- compared to WA314 infected macrophages and this could be prevented by MAP-kinase inhibitors (S5E Fig). In the WA314ΔYopP infected macrophages ABI1 prominently accumulated at cell cell contacts, where it colocalized with actin, vinculin and the zonula occludens protein ZO1 (Figs 7G, H). Further, accumulation of ABI1 was associated with

increased levels of actin at the cell cell contacts, indicating enhanced WAVE regulatory complex-induced actin polymerization (Figs 7G, H; Yamazaki et al., 2007). Altogether this data shows that the histone modification-driven reprogramming of ABI1 gene expression in fact can alter actin cytoskeleton organization in *Yersinia* infected macrophages.

Discussion

At present only scarce information is available on epigenetic reprogramming of immune cells by pathogenic bacteria (Rolando et al., 2013; Pacis et al., 2019). This study was conducted to find out whether the entero-pathogen *Y. enterocolitica* alters chromatin states to globally control gene expression in human macrophages. Our results provide a number of novel insights into systemic reorganization of epigenetic histone modifications in human macrophages by pathogenic yersiniae.

A primary goal was to map in detail whether and how the effects of the *Yersinia* PAMPs on histone modifications are reorganized by the T3SS associated virulence factors of the bacteria. To this end, we systematically compared the effects of a *Y. enterocolitica* wild type strain and a derived avirulent strain.

Virulent and avirulent yersiniae extensively reorganized histone marks (H3K4me1, H3K4me3 and H3K27ac) at macrophage gene promoters and enhancers. H3K27ac marks were the most dynamic (> 22.000 loci altered) followed by H3K4me3 marks (1600 loci altered). That H3K27ac marks are highly dynamic in human macrophages stimulated with bacterial agents has been reported previously (Novakovic et al., 2016).

We could classify the bacterial reorganization of histone modifications in four profiles, which we named Suppression, Down, Up and Prevention. In the Suppression- and Prevention profiles, the bacteria's T3SS effectors block the PAMP-induced deposition or removal, respectively, of histone marks. In Down- and Up profiles, the T3SS-associated effectors down- or up-regulate, respectively, histone marks independently of PAMP activities.

The fraction of histone modifications overlapping with actual gene expression in the four profiles varied widely. Overlaps ranged from 30 % in the Suppression profile to 2% in the Down profile. The biological significance of *Yersinia*-modulated histone modifications that do not immediately affect gene expression is unclear. These "silent" histone modifications

may be involved in priming, immune memory, immune tolerance or other complex gene regulatory processes in macrophages (Glass & Natoli, 2015; Ivashkiv, 2013).

It was interesting to note that different histone marks at individual promoters or at related promoters and enhancers were reorganized in a coordinated manner by the bacteria, mostly in the Suppression- and Prevention profiles. In these instances, the histone modifications were more frequently associated with changes in gene expression. Thus, the bacterial pathogenicity factors systematically co-regulate different histone modifications to effectively act on gene transcription.

The T3SS effector YopP accounted for 40-50% of the changes in histone modifications and gene expression produced by virulent *Y. enterocolitica* in macrophages, as exemplified with inflammatory and Rho GTPase pathway genes. Inhibition of MAP-kinase signaling was a crucial mechanism underlying these YopP effects. YopP regulated the expression of genes, at which it changed histone modifications, to very different degrees. E.g., for individual inflammatory or Rho GTPase pathway genes the contribution of YopP to the *Yersinia* effect ranged from null to 100%. Interestingly, the histone modifications at some of the genes whose expression was strongly affected by YopP were changed by other T3SS effectors. We could exclude YopM as one of these effectors, because it did not alter any of the histone modifications investigated here. Thus, YopP but not YopM regulates the expression of selective genes through histone modifications and thereby seemingly cooperates to varying extents with other T3SS effectors. Of note, in addition to histone modifications, other gene regulatory mechanisms clearly also contribute to the *Yersinia*- and YopP effects on gene expression (Köberle et al., 2012). Thus, our data suggest that virulent yersiniae fine tune expression of individual genes in specific biological pathways through governing the cooperation between histone modifications and other gene regulatory mechanisms. For this the bacteria employ YopP as the main T3SS effector that cooperates with other effectors.

Together the effectors mostly remodel PAMP-induced signal transduction but also exert PAMP independent effects on gene transcription (Köberle et al., 2012).

Among the most significant findings of our study was the remodeling of histone modifications at 61 % of all 534 known Rho GTPase genes. When considered in terms of gene expression, 38 % of all known Rho GTPase pathway genes were differentially expressed whereby well over half of them were associated with dynamic histone modifications. The latter encode Rho proteins (Rho GTPases) and their effectors, activators (GEFs) and deactivators (GAPs). To control dynamic cellular processes such as cytoskeletal reorganization or vesicular transport, the right Rho proteins, regulators and effectors have to be activated or deactivated at the right time and location. Rho GTPase signaling networks are characterized by the sheer countless interactions that can take place between the different Rho GTPases, regulators and effectors and by crosstalk and feedback loops (Bustelo et al., 2007; Paul et al., 2017; Bagci et al., 2020; Müller et al., 2020). Our results add a further level of complexity to Rho GTPase regulation in macrophages by revealing an extensive epigenetic control of Rho GTPase pathway gene expression.

One of our intriguing findings was that genes encoding GAPs for Rac were overrepresented in the Prevention profile. This indicates that by epigenetic regulation *Yersinia* creates a cellular state in which downregulation of Rac inhibitors is prevented, which favours Rac inhibition. Inhibition of Rac is a known central strategy of *Yersinia* with the three T3SS effectors YopE, YopT and YopO acting as Rac inhibitors (Aepfelbacher & Wolters, 2017). Further consistent with this bacterial strategy is the finding that expression of Rac1, the Rac1 activator RhoG and the atypical Rho proteins RhoH and RhoU, which can take over Rac functions, were suppressed by the bacteria (Bagci et al., 2020; Aspenström et al., 2007; Hodge & Ridley, 2016; Tajadura-Ortega et al.,2018; Chardin, 2006). A reason why *Yersinia* places a focus on inhibition of Rac may be the outstanding role that it plays in anti-microbial activities of macrophages such as phagocytosis, chemotaxis and production of reactive oxygen species

(Bokoch, 2005). Rac inhibition by YopE also prevents overshooting translocation of T3SS effectors into cells (Aepfelbacher & Wolters, 2017). A number of genes for atypical Rho proteins (RHOH, RHOU, RND1, RHOBTB1, RHOBTB2) were found in the Suppression and Prevention profiles. The activities of atypical Rho proteins are generally controlled by gene transcription and protein degradation and not by GAPs and GEFs (Aspenström et al., 2007; Haga & Ridley, 2016), but their regulation by epigenetic mechanisms has so far not been reported. Although the specific functions of atypical Rho proteins in macrophages are widely unknown, atypical Rho proteins also can regulate the activity of classical Rho proteins in different cell types (Aspenström et al., 2007; Stiegler & Boggon, 2020; Hodge & Ridley, 2016; Chardin, 2006). For instance, RhoH spatially controls Rac1 activity (Tajadura-Ortega et al.,2018) and Rnd proteins bind and steer Rho GAP proteins to specific cell sites (Stiegler & Boggon, 2020). We also found that downregulation of genes for the atypical Rho proteins RhoBTBs was prevented and expression of genes for some RhoBTB effectors was suppressed in parallel by the bacteria. Thus, through epigenetic mechanisms *Yersinia* may determine which atypical Rho protein/effector pairs are functional in macrophages. Considering the universal role that Rho GTPases play in cellular function, the multifaceted epigenetic regulation of their expression will undoubtedly affect their activities and thereby have functional consequences in macrophages.

Providing evidence for this notion, we here show that histone modification driven ABI1 gene expression affects accumulation of the ABI1 protein, a component of the WAVE actin regulatory complex, at macrophage-macrophage contacts. Increased ABI1 enhances actin accumulation and recruitment of adhesion proteins at these contacts, likely promoting the stabilization of these structures (Ryu et al., 2009; Zipfel et al., 2006).

Taken together, in this study we decipher key principles of epigenetic reprogramming of human macrophages by the bacterial entero-pathogen *Y. enterocolitica*. 1) Remodeling of histone modifications and associated changes in gene expression can be classified in different

profiles, with virulent bacteria mainly suppressing or preventing the effects of bacterial PAMPs, but also exerting independent stimulatory or inhibitory activities through their T3SS effectors. Suppressed histone modifications with corresponding gene suppression mostly belong to immune and inflammatory signaling, whereas prevented modifications/genes belong to Rho GTPase pathway and metabolic pathways. 2) Changes in the different histone modifications at promoters and enhancers are often coordinated, so that they can act cooperatively on gene expression. 3) The T3SS effector YopP contributes up to 50 % to *Yersinia*-induced remodeling of histone modifications and gene expression, through its inhibitory effect on MAP kinase signaling. At the level of individual gene expression, the contribution of YopP varies from null to 100%, even in genes belonging to the same biological pathways. 4) Histone modifications, transcription factor expression, and other unidentified mechanisms are reprogrammed by YopP and other T3SS effectors and cooperatively cause the effects of *Yersinia* on individual gene expression. 5) While there was an up to 30% overlap between histone modifications and associated gene expression in the profiles, the majority of histone modifications did not alter gene expression. In these cases, such epigenetic modifications could prepare cells for subsequent stimuli or provide a basis for innate immune memory or tolerance. Further studies are warranted to test these intriguing possibilities.

Materials and Methods

Cell culture

Human peripheral blood monocytes were isolated from buffy coats as described in Kopp et al., 2006. Cells were cultured in RPMI1640 containing 20 % autologous serum at 37 °C and 5 % CO_2 atmosphere. The medium was changed every three days until cells were differentiated into macrophages after 7 days. Macrophages were used for infection 1-2 weeks after the isolation.

Infection of cells

On the day before infection of primary human macrophages the cell medium was changed to RPMI1640 without antibiotics and serum and precultures of *Y. enterocolitica* strains (S1 Table) were grown overnight in LB medium with appropriate antibiotics at 27 °C and 200 x rpm. On the day of infection precultures were diluted 1:20 in fresh LB medium without antibiotics and incubated for 90 min at 37 °C and 200 x rpm to induce activation of the *Yersinia* T3SS machinery and Yop expression. Afterwards bacteria were pelleted by centrifugation for 10 min at 6000 x g, 4 °C and resuspended in 1 ml ice-cold PBS containing 1 mM $MgCl_2$ and $CaCl_2$. The optical density OD_{600} was adjusted to 3.6 and afterwards macrophages were infected at multiplicity-of-infection (MOI) of 100. Cell culture dishes were centrifuged for 2 min at RT and 200 x g to sediment bacteria on the cells and synchronize infection. Cells were incubated at 37 °C for 6 h.

Treatment with MAPK inhibitors

For the MAPK pathway inhibition combination of 5 μM SB203580 (Cayman Chemical) and 5 μM PD98059 (Merck Millipore), which target p38 and MEK1, respectively, was used. Inhibitors were added to macrophages 30-60 min before the infection.

RNA-seq

Total RNA of 1-2 x 10^6 human macrophages was isolated using RNeasy extraction kit (Qiagen) including DNAse treatment according to manufacturer's instructions. RNA integrity of the isolated RNA was analysed with the RNA 6000 Nano Chip (Agilent Technologies) on an Agilent 2100 Bioanalyzer (Agilent Technologies). mRNA was extracted using the NEBNext Poly(A) mRNA Magnetic Isolation module (New England

Biolabs) and RNA-seq libraries were generated using the NEBNext Ultra RNA Library Prep Kit for Illumina (New England Biolabs) as per manufacturer's recommendations. Concentrations of all samples were measured with a Qubit 2.0 Fluorometer (Thermo Fisher Scientific) and fragment lengths distribution of the final libraries was analysed with the DNA High Sensitivity Chip (Agilent Technologies) on an Agilent 2100 Bioanalyzer (Agilent Technologies). All samples were normalized to 2 nM and pooled equimolar. The library pool was sequenced on the NextSeq500 (Illumina) with 1 x 75 bp and total 19.9 to 23.8 million reads per sample.

RNA-seq analysis

Sequencing reads containing bases with low quality scores (quality Phred score cutoff 20) or adapters were trimmed using TrimGalore program (http://www.bioinformatics.babraham.ac.uk/projects/trim_galore/).

Reads were aligned to the human reference assembly hg19 using STAR (Dobin et al., 2012). FeatureCounts (Liao et al., 2014) was employed to obtain the number of reads mapping to each gene.

RNA-seq data have been deposited in the ArrayExpress database at EMBL-EBI (www.ebi.ac.uk/arrayexpress) under accession number E-MTAB-10473. RNA-seq data from additional replicates of mock, WA314 6h and WA314ΔYopM 6h were obtained from European Nucleotide Archive (ENA) at http://www.ebi.ac.uk/ena/data/view/PRJEB10086.

RNA-seq differential expression analysis

Statistical analysis of differential expression was carried out with DESeq2 (Love et al., 2014) using raw counts as an input and the experimental design *~batch + condition*. Significantly

enriched genes were defined with fold change ≥ 2 and adjusted P-value ≤ 0.05. Normalized rlog counts for each gene were obtained after batch effect removal with limma package (Ritchie et al., 2015) and used for downstream clustering analysis and visualization. Reproducibility between replicates was confirmed by PCA analysis and sample distance heatmaps.

Clustering analysis of all DEGs from comparisons between mock, WAC, WA314 was done with rlog counts in R with pheatmap package. Clustering was performed with clustering distance based on Euclidean distance and Complete clustering method to yield 6 clusters which were further assembled into profiles Suppression, Prevention, Up and Down. Clustering distance, clustering method and number of clusters were selected so that all meaningful clusters were identified by the analysis. For heatmaps rlog counts from DESeq2 analysis were scaled by row (row Z-score) and low to high expression levels are indicated by blue-white-red color gradient. 2 representative replicates are shown for each sample.

Chromatin immunoprecipitation (ChIP)

For the ChIP with formaldehyde crosslinking, macrophages (3-10 x 10^6 cells per condition) were washed once with warm PBS and incubated for 30 min at 37 °C with accutase (eBioscience) to detach the cells. ChIP protocol steps were performed as described in (Günther et al., 2016), except that BSA-blocked ChIP grade protein A/G magnetic beads (Thermo Fisher Scientific) were added to the chromatin and antibody mixture and incubated for 2 h at 4 °C rotating to bind chromatin-antibody complexes. Samples were incubated for ~3 min with a magnetic stand to ensure attachment of beads to the magnet and mixed by pipetting during the wash steps. Eluted DNA was either subjected to ChIP-seq library preparation or used for ChIP-qPCR experiments. Input chromatin DNA was prepared from 1/4 of chromatin amount used for ChIP. Antibodies used for ChIP were anti-H3K4me3 (Merck Millipore, 04–745, 4 µl per ChIP), anti-H3K27me3 (Merck Millipore, 07-449, 4 µl

per ChIP), anti-H3K27ac (abcam, ab4729, 4 µg per ChIP) and anti-H3K4me1 (Cell Signaling, 5326S, 5 µl per ChIP).

ChIP library preparation and sequencing

ChIP-seq libraries were constructed with 1-10 ng of ChIP DNA or input control as a starting material. Libraries were generated using the NEXTflex™ ChIP-Seq Kit (Bioo Scientific) as per manufacturer's recommendations. Concentrations of all samples were measured with a Qubit Fluorometer (Thermo Fisher Scientific) and fragment length distribution of the final libraries was analysed with the DNA High Sensitivity Chip on an Agilent 2100 Bioanalyzer (Agilent Technologies). All samples were normalized to 2 nM and pooled equimolar. The library pool was sequenced on the NextSeq500 (Illumina) with 1 x 75 bp and total 18.6 to 41 million reads per sample.

ChIP-seq analysis

Sequencing reads containing bases with low quality scores (quality Phred score cutoff 20) or adapters were trimmed using TrimGalore program (http://www.bioinformatics.babraham.ac.uk/projects/trim_galore/).

BWA (Li & Durbin, 2009) was used to align reads from FASTQ files to hg19 human reference genome. Samtools (Liet et al., 2009) was used for manipulations (e.g. sorting, indexing, conversions) of the sequencing files. Picard (https://broadinstitute.github.io/picard/) was used for duplicate read removal. BEDTools (Quinlan & Hall, 2010) was used for generation of BED files. The following command was used for the alignment to hg19:

bwa mem -M <reference genome> <ChIP-seqfile.fastq> | samtools view -bT <reference genome> | samtools view -b -q 30 -F 4 -F 256 > <aligned-ChIP-seq-file.bam>

ChIP-seq data have been deposited in the ArrayExpress database at EMBL-EBI (www.ebi.ac.uk/arrayexpress) under accession number E-MTAB-10475.

ChIP-seq peak calling

MACS2 peak calling (Zhang et al., 2008) against the input control was used for H3K4me3 and H3K27ac with *-q 0.01* parameter. SICER peak calling (Zang et al., 2009) against the input control was used for H3K4me1 and H3K27me3 with default settings. SICER peaks for ChIP enrichment over background with fold change ≥ 2 were selected. MACS2 and SICER peaks were filtered to exclude blacklisted regions (Amemiya et al., 2019). To generate a file with all peaks for each modification, peaks found in replicates for different conditions were pooled together and merged using BEDTools (Quinlan & Hall, 2010).

ChIP-seq differential region analysis

DiffReps (Shen et al., 2013) was used for identification of differentially enriched regions/ dynamic regions between mock, WAC and WA314. Csaw (Lun & Smyth, 2015; *width 150, spacing 100, minq 50, ext 210*) normalization coefficients for efficiency bias were used as input to normalize the data in diffReps. Other diffReps parameters were set to default except for H3K4me1 and H3K27me3 where *–nsd broad* parameter was used. Accuracy of differentially enriched regions was examined in IGV (Thorvaldsdóttir et al., 2012). Significant sites with log2 FC ≥ 1 and adjusted P-value ≤ 0.05 were selected. Regions were further filtered to exclude regions that do not overlap MACS2 or SICER peaks, overlap blacklist regions (Amemiya et al., 2019) and regions with low read counts (less than 20 for any replicate in the upregulated condition; less than 20 in the upregulated condition for H3K4me3). Additionally, H3K27me3 regions with length less than 1700 bp were excluded as smaller regions appeared to be false positives. For further clustering analysis of H3K4me3

and H3K27ac dynamic regions at promoters and enhancers all differential sites for each mark for different conditions were pooled together and merged.

ChIP-seq quantification of tag counts

For quantification of tag counts at peaks and differential sites raw counts at target regions were quantified using EaSeq (Lerdrup et al., 2016) and normalized with csaw (Lun & Smyth, 2015; *width 150, spacing 100, minq 50, ext 210*) efficiency bias coefficients with the formula: *(1+raw counts)/(csaw effective library size/10^6)/bp per kb*.

ChIP-seq classification and annotation of regions

Promoter coordinates of ±2 kb from TSS and associated gene annotations were extracted from RefSeq hg19 gene annotations in UCSC Genome Browser (Haeussler et al., 2018) using EaSeq (Lerdrup et al., 2016). Regions overlapping promoter coordinates were defined as regions at promoters and annotated with associated genes; one region could overlap multiple promoters and associate with multiple genes. Regions that did not overlap promoters but overlapped with H3K4me1 regions were assigned to enhancers. Enhancer regions were annotated to the closest gene in EaSeq. The remaining regions were classified as “undefined”. For the identification of “dynamic” and “constant” peak regions, pooled peaks (based on MACS2 or SICER) were intersected with pooled differential site regions (based on diffReps) for each histone modification. Peaks intersecting differential regions were defined as “dynamic”, whereas the rest of the peaks were termed “constant”.

Latent enhancers were defined as sites outside promoters with H3K4me1 signal increase based on diffReps without pre-existing H3K4me1 signal (no SICER peaks)

ChIP-seq clustering of promoters and enhancer regions

Clustering of normalized tag counts at pooled differential sites was performed with R function heatmap.2. All H3K4me3 and H3K27ac regions from pooled differential sites that intersected promoter regions were used for promoter (P1a-P2d classes) heatmaps. For the H3K27ac enhancer heatmap (E1-E4 classes) all H3K27ac regions from pooled differential sites outside promoters and overlapping H3K4me1 peaks were used. H3K4me3 promoter heatmap was generated with clustering distance based on Pearson correlation and Complete clustering method. For H3K27ac promoter heatmap regions which did not overlap regions in H3K4me3 promoter heatmap were used for clustering. H3K27ac promoter and enhancer heatmaps were generated with clustering distance based on Spearman correlation and Average clustering method. Clustering distance, clustering method and number of clusters were selected so that all meaningful clusters were identified by the analysis. Clusters were further assembled into classes based on the pattern of histone modifications across conditions.

ChIP-seq comparison to public data

For comparison of H3K27ac data from this study and publicly available data (Park et al., 2017; Novakovic et al., 2016) raw tag counts at all H3K27ac peaks from this study were normalized with csaw (Lun & Smyth, 2015) efficiency bias coefficients. Batch effect between different datasets was removed using limma package (Ritchie et al., 2015) and tag counts used to calculate Spearman correlation.

ChIP-qPCR

ChIP-qPCR was performed with SYBR Green/ROX qPCR Master Mix kit (Thermo Fisher Scientific) following manufacturer's instructions. Primers (S15 Table) were designed using PRIMER-Blast tool (Ye et al., 2012) with the optimal melting temperature of 60 °C and template length between 55 and 200 bp. For all primer pairs input chromatin DNA was used

to generate standard curves and verify amplification efficiency between 90-100 %. The specificity of primers was confirmed using reaction without a DNA template and melting curve analysis of PCR products. qPCR was performed on a Rotorgene 6000 qPCR machine (Qiagen) and analysed with the Rotor-Gene 6000 software (Qiagen). A gain optimization was carried out at the beginning of the run. Concentration of amplified DNA was calculated based on the standard curve. In order to compare changes in enrichment at specific regions between different conditions, normalization was done with at least 2 selected control regions which did not show change in histone modifications during infection.

Pathway analysis

Gene Ontology (GO) and Kyoto Encyclopedia of Genes and Genomes (KEGG) terms were determined for RNA-seq and ChIP-seq gene lists by using DAVID webtool (Huang et al., 2008; Huang et al., 2009).

Motif analysis

TF motif enrichment for known motifs was performed using HOMER package (Heinz et al., 2010). Command *findMotifsGenome.pl* was used and a list of genomic coordinates was supplied as an input; the exact size of supplied regions was used by setting parameter *-size given*.

Boxplots

Boxplots were generated using ggplot2 in R. Boxes encompass the twenty-fifth to seventy-fifth percentile changes. Whiskers extend to the tenth and ninetieth percentiles. Outliers are depicted with black dots. The central horizontal bar indicates the median.

Association between RNA-seq and ChIP-seq

Gene lists from RNA-seq and ChIP-seq were compared based on gene symbols to find the number of overlapping genes and determine how many genes showed associated epigenetic and gene expression changes. In some cases RNA-seq lists contained old gene symbols which did not match to symbols in ChIP-seq lists with RefSeq annotation from UCSC. All old symbols in RNA-seq lists without a match in RefSeq annotation were replaced with the new symbol using Multi-symbol checker tool (Braschi et al., 2019).
Relative overlap between promoter and enhancer classes was obtained by dividing the number of overlapping genes from two input classes with the total number of genes from the first input class and then with total number of genes from the second input class.

Calculation of % YopP effect

Percentage YopP effect was calculated as ratio of FC between WA314ΔYopP vs WA314 and WAC vs WA314 (Suppression and Prevention) or WA314 vs mock (Up and Down). % YopP effect was presented for individual strongly WA314-regulated genes and regions from inflammatory response and Rho GTPase pathway, which associated with gene expression and histone modification changes in Suppression and Prevention profiles. Specifically, only genes were selected, which overlapped WAC vs WA314 DEGs and differentially enriched regions. Normalized tag counts were calculated for the target regions and used to obtain FC.

Rho GTPase pathway gene analysis

The target gene list with 534 Rho GTPase pathway genes was compiled from publicly available data and included 370 effectors binding GTP-Rho GTPases (Bustelo et al., 2007; Bagci et al., 2020; Paul et al., 2017), 66 GAPs, 77 GEFs (Müller et al., 2020) and 23 Rho

GTPases (Wennerberg & Der, 2004; Senoo et al., 2019 list in the supplementary). The list of genes does not match the list together with activities (534 vs 536) as some genes possess multiple activities.

Immunofluorescence staining

Infected cells were washed twice with PBS, fixed with 4 % PFA in PBS for 5 min and permeabilized with 0.1 % Triton X-100 (w/v) in PBS for 10 min. After fixation and permeabilization coverslips were washed twice with PBS. Unspecific binding sites were blocked with 3 % bovine serum albumin (BSA, w/v) in PBS for at least 30 min. Samples were then incubated with 1:100 (anti-ABI1 (Sigma-Aldrich), anti-ZO-1 (Zymed)) or 1:200 (anti-vinculin (Sigmal-Aldrich)) dilution of the primary antibody for 1 h and incubated with a 1:200 dilution of the suitable fluorophore-coupled secondary antibody for 45 min. Secondary anti-IgG antibodies and dyes used: Alexa488 chicken anti-rabbit (Molecular Probes), Alexa568 goat anti-mouse (Molecular Probes), AlexaFluor568 phalloidin (Invitrogen, GIBCO), AlexaFluor633 phalloidin (Invitrogen, GIBCO).

After each staining coverslips were washed three times with PBS. Both, primary and secondary antibodies were applied in PBS supplemented with 3 % BSA. Fluorophore-coupled phalloidin (1:200, Invitrogen) was added to the secondary antibody staining solution as indicated. Coverslips were mounted in ProLong Diamond (Thermo Fisher Scientific).

Microscopy

Fixed samples were analyzed with a confocal laser scanning microscope (Leica TCS SP8) equipped with a 63x, NA1.4 oil immersion objective and Leica LAS X SP8 software (Leica Microsystems, Wetzlar, Germany) was used for acquisition.

Image analysis

The z-stacks of images were combined to one image using maximum intensity projection. These images were used to measure the mean fluorescent intensity of the F-actin signal with a circle (9.02 µm diameter) around the cellular junctions between macrophages. The signal intensity at junctions refers to the maximum value of 255 for 8-bit images.

Western blot analysis

Primary human macrophages (1-2*10^6 cells per condition) were washed once with warm PBS and scrapped off the plates to harvest the cells. Cell were pelleted by centrifugation at 700 x g, 10 min and 4°C. Cells were resuspended in 60 µl Lysis buffer (50 mM HEPES-KOH, pH 7.5,

140 mM NaCl, 1 mM EDTA, 10 % glycerol, 0.5 % NP-40, 0.75 % Triton X-100, protease inhibitor (Complete, Roche Diagnostics) and lysed by incubation at 4°C for 30 min. Lysate was centrifuged at 10000 x g, 10 min and 4°C and supernantant was collected for Western blot analysis.

Proteins were separated by SDS-PAGE and transferred to polyvinylidene difluoride (PVDF) membrane (Immobilion-P, Millipore) by semi-dry blotting. The membrane was incubated in blocking solution (5 % milk powder (w/v) in TBS supplemented with 0.03 % Tween 20; TBS-T) at room temperature for 30 min. Primary antibody incubations (anti-ABI1 (Sigma-Aldrich) at 1:1000, anti-GAPDH (Sigma-Aldrich) at 1:3000) were carried out at 4°C overnight, secondary antibody incubation (horseradish peroxidase linked anti-rabbit IgG (Cell signaling) at 1:10000) was performed at room temperature for 1 h. Washing steps with TBS-T were done between incubations. Antibody signals were visualized with chemiluminescence technology (Supersignal West Femto, Pierce Chemical) and captured on X-ray films (Fujifilm).

Ethics statement

Approval for the analysis of anonymized blood donations (WF-015/12) was obtained by the Ethical Committee of the Ärztekammer Hamburg (Germany).

Acknowledgements

We thank the UKE Core Facility Microscopy Imaging (Umif) for help with experimental setups and data analysis. We also would like to thank Daniela Indenbirken for generating the RNA-seq libraries and Frank Bentzien (UKE Transfusion Medicine) for buffy coats.

References

1. Aepfelbacher, M. & Wolters, M. in The Actin Cytoskeleton and Bacterial Infection 201–220 (Springer International Publishing, Cham, 2017).

2. Aktories, K., Schmidt, G. & Just, I. Rho GTPases as Targets of Bacterial Protein Toxins. Biological Chemistry **381,** 421 –426 (2000).

3. Aktories, K. Bacterial protein toxins that modify host regulatory GTPases. Nature reviews. Microbiology **9,** 487—498 (2011).

4. Allis, C. D. & Jenuwein, T. The molecular hallmarks of epigenetic control. Nature Reviews Genetics **17,** 487–500 (2016).

5. Amemiya, H. M., Kundaje, A. & Boyle, A. P. The ENCODE Blacklist: Identification of Problematic

Regions of the Genome. Scientific Reports **9,** 9354 (2019).

6. Aspenström, P., Ruusala, A. & Pacholsky, D. Taking Rho GTPases to the next level: The cellular functions of atypical Rho GTPases. Experimental Cell Research **313,** 3673 –3679 (2007).

7. Bagci, H. et al. Mapping the proximity interaction network of the Rho-family GTPases reveals signalling pathways and regulatory mechanisms. Nature cell biology **22,** 120—134 (2020).

8. Balada-Llasat, J.-M. & Mecsas, J. Yersinia Has a Tropism for B and T Cell Zones of Lymph Nodes That Is Independent of the Type III Secretion System. PLOS Pathogens **2,** 1–13 (2006).

9. Barski, A. et al. High-Resolution Profiling of Histone Methylations in the Human Genome. Cell **129,** 823—837 (2007).

10. Bedi, R., Du, J., Sharma, A. K., Gomes, I. & Ackerman, S. J. Human C/EBP-E activator and repressor isoforms differentially reprogram myeloid lineage commitment and differentiation. Blood **113,** 317–327 (2009).

11. Berneking, L. et al. Immunosuppressive Yersinia Effector YopM Binds DEAD Box Helicase DDX3 to Control Ribosomal S6 Kinase in the Nucleus of Host Cells. PLoS Pathogens **12,** 1–35 (2016).

12. Bierne, H., Hamon, M. & Cossart, P. Epigenetics and Bacterial Infections. Cold Spring Harbor Perspectives in Medicine **2** (2012).

13. Bokoch, G. M. Regulation of innate immunity by Rho GTPases. Trends in Cell Biology **15,** 163–171 (2005).

14. Boureux, A., Vignal, E., Faure, S. & Fort, P. Evolution of the Rho Family of Ras-Like GTPases in Eukaryotes. Molecular Biology and Evolution **24,** 203–216 (2006).

15. Braschi, B. et al. Genenames.org: the HGNC and VGNC resources in 2019. Nucleic Acids Research **47,** D786–D792 (2018).

16. Brodsky, I. E. et al. A Yersinia Effector Protein Promotes Virulence by Preventing Inflammasome Recognition of the Type III Secretion System. Cell Host and Microbe **7,** 376 –387 (2010).

17. Broz, P. & Dixit, V. M. Inflammasomes: mechanism of assembly, regulation and signalling. Nature reviews. Immunology **16,** 407—420 (2016).

18. Bustelo, X. R., Sauzeau, V. & Berenjeno, I. M. GTP-binding proteins of the Rho/Rac family: regulation, effectors and functions in vivo. BioEssays **29,** 356–370 (2007).

19. Chardin, P. Function and regulation of Rnd proteins. Nature reviews. Molecular cell biology **7,** 54—62 (2006).

20. Chen, B. et al. Epigenetic activation of the small GTPase TCL contributes to colorectal cancer cell migration and invasion. Oncogenesis **9,** 86 (2020).

21. Chen, X. et al. Ena/VASP Proteins Cooperate with the WAVE Complex to Regulate the Actin Cytoskeleton. Developmental Cell **30,** 569–584 (2014).

22. Christgen, S., Place, D. E. & Kanneganti, T.-D. Toward targeting inflammasomes: insights into their regulation and activation. Cell research **30,** 315—327 (2020).

23. Chung, L. K. et al. The Yersinia Virulence Factor YopM Hijacks Host Kinases to Inhibit Type III Effector-Triggered Activation of the Pyrin Inflammasome. Cell Host and Microbe **20,** 296 –306 (2016).

24. Connor, M., Arbibe, L. & Hamon, M. Customizing Host Chromatin: a Bacterial Tale. Microbiology Spectrum **7** (2019).

25. Cornelis, G. R. & Wolf-Watz, H. The Yersinia Yop virulon: a bacterial system for subverting eukaryotic cells. Molecular Microbiology **23,** 861–867 (1997).

26. Diacovich, L. & Gorvel, J.-P. Bacterial manipulation of innate immunity to promote infection.

Nature Reviews Microbiology **8,** 117–128 (2010).

27. Dobin, A. et al. STAR: ultrafast universal RNA-seq aligner. Bioinformatics **29,** 15–21 (2012).

28. Dong, W. & Hamon, M. A. Revealing eukaryotic histone-modifying mechanisms through bacterial infection. Seminars in Immunopathology **42,** 201–213 (2020).

29. Doyle, S. E. et al. Toll-like Receptors Induce a Phagocytic Gene Program through p38. Journal of Experimental Medicine **199,** 81–90 (2004).

30. Fritz, G., Just, I. & Kaina, B. Rho GTPases are over-expressed in human tumors. International Journal of Cancer **81,** 682–687 (1999).

31. Gallant, S. & Gilkeson, G. ETS transcription factors and regulation of immunity. Archivum Immunologiae et Therapiae Experimentalis **54,** 149–163 (2006).

32. Galán, J. E. & Wolf-Watz, H. Protein delivery into eukaryotic cells by type III secretion machines. Nature **444,** 567—573 (2006).

33. Gao, P. et al. Transcription factor Fli-1 positively regulates lipopolysaccharide-induced interleukin-27 production in macrophages. Molecular immunology **71,** 184—191 (2016).

34. Glass, C. K. & Natoli, G. Molecular control of activation and priming in macrophages. Nature immunology **17,** 26–33 (2015).

35. Günther, T., Theiss, J. M., Fischer, N. & Grundhoff, A. Investigation of Viral and Host Chromatin by ChIP-PCR or ChIP-Seq Analysis. Current Protocols in Microbiology **40,** 1E.10.1–1E.10.21 (2016).

36. Göös, H. et al. Gain-of-function CEBPE mutation causes noncanonical autoinflammatory inflammasomopathy. Journal of Allergy and Clinical Immunology **144,** 1364–1376 (2019).

37. Haeussler, M. et al. The UCSC Genome Browser database: 2019 update. Nucleic Acids Research **47,** D853–D858 (2018).

38. Haga, R. B. & Ridley, A. J. Rho GTPases: Regulation and roles in cancer cell biology. Small GTPases **7,** 207–221 (2016).

39. Heasman, S. J. & Ridley, A. J. Mammalian Rho GTPases: new insights into their functions from in vivo studies. Nature reviews. Molecular cell biology **9,** 690—701 (2008).

40. Heintzman, N. D. et al. Histone modifications at human enhancers reflect global cell type-specific gene expression. Nature **459,** 108–112 (2009).

41. Heinz, S. et al. Simple Combinations of Lineage-Determining Transcription Factors Prime cis-Regulatory Elements Required for Macrophage and B Cell Identities. Molecular Cell **38,** 576–589 (2010).

42. Hodge, R. G. & Ridley, A. J. Regulating Rho GTPases and their regulators. Nature reviews. Molecular cell biology **17,** 496—510 (2016).

43. Hoffmann, R., Van Erp, K., Trülzsch, K. & Heesemann, J. Transcriptional responses of murine macrophages to infection with Yersinia enterocolitica. Cellular Microbiology **6,** 377–390 (2004).

44. Hop, H. T. et al. The Key Role of c-Fos for Immune Regulation and Bacterial Dissemination in Brucella Infected Macrophage. Frontiers in Cellular and Infection Microbiology **8,** 287 (2018).

45. Huang, D. W., Sherman, B. T. & Lempicki, R. A. Bioinformatics enrichment tools: paths toward the comprehensive functional analysis of large gene lists. Nucleic Acids Research **37,** 1–13 (2008).

46. Huang, D. W., Sherman, B. T. & Lempicki, R. A. Systematic and integrative analysis of large gene lists using DAVID bioinformatics resources. Nature Protocols **4,** 44–57 (2009).

47. Ivashkiv, L. B. Epigenetic regulation of macrophage polarization and function. Trends in Immunology **34,** 216 –223 (2013).

48. Jaffe, A. B. & Hall, A. RHO GTPASES: Biochemistry and Biology. Annual Review of Cell and Developmental Biology **21,** 247–269 (2005).

49. Kang, K. et al. IFN- selectively suppresses a subset of TLR4-activated genes and enhancers to potentiate macrophage activation. Nature Communications **10** (2019).

50. Köberle, M. et al. Yersinia enterocolitica YopT and Clostridium difficile Toxin B Induce Expression of GILZ in Epithelial Cells. PLOS ONE **7,** 1–17 (2012).

51. Klemm, S. L., Shipony, Z. & Greenleaf,W. J. Chromatin accessibility and the regulatory epigenome. Nature reviews. Genetics **20,** 207—220 (2019).

52. Kopp, P. et al. The Kinesin KIF1C and Microtubule Plus Ends Regulate Podosome Dynamics in Macrophages. Molecular Biology of the Cell **17,** 2811–2823 (2006).

53. Laurin, M. & Côté, J.-F. Insights into the biological functions of Dock family guanine nucleotide exchange factors. Genes and Development **28,** 533–547 (2014).

54. Lennard Richard, M. L. et al. The Fli-1 transcription factor regulates the expression of CCL5/RANTES. Journal of immunology (Baltimore, Md. : 1950) **193,** 2661—2668 (2014).

55. Lerdrup, M., Johansen, J. V., Agrawal-Singh, S. & Hansen, K. An interactive environment for agile analysis and visualization of ChIP-sequencing data. Nature Structural & Molecular Biology **23,** 349–357 (2016).

56. Li, H. & Durbin, R. Fast and accurate short read alignment with Burrows–Wheeler transform. Bioinformatics **25,** 1754–1760 (2009).

57. Li, H. et al. The Sequence Alignment/Map format and SAMtools. Bioinformatics **25,** 2078–2079 (2009).

58. Liao, Y., Smyth, G. K. & Shi, W. featureCounts: an efficient general purpose program for assigning sequence reads to genomic features. Bioinformatics (Oxford, England) **30,** 923—930 (2014).

59. Love, M. I., Huber, W. & Anders, S. Moderated estimation of fold change and dispersion for RNA-seq data with DESeq2. Genome Biology **15,** 550 (2014).

60. Lun, A. T. & Smyth, G. K. csaw: a Bioconductor package for differential binding analysis of ChIP-seq data using sliding windows. Nucleic Acids Research **44,** e45–e45 (2015).

61. Lupfer, C., Malik, A. & Kanneganti, T.-D. Inflammasome control of viral infection. Current Opinion in Virology **12.** Antiviral strategies • Virus structure and expression, 38 –46 (2015).

62. Malsin, E. S., Kim, S., Lam, A. P. & Gottardi, C. J. Macrophages as a Source and Recipient of Wnt Signals. Frontiers in Immunology **10,** 1813 (2019).

63. Marketon, M. M., DePaolo, R. W., DeBord, K. L., Jabri, B. & Schneewind, O. Plague Bacteria Target Immune Cells During Infection. Science **309,** 1739–1741 (2005).

64. McPhee, J. B., Mena, P., Zhang, Y. & Bliska, J. B. Interleukin-10 Induction Is an Important Virulence Function of the Yersinia pseudotuberculosis Type III Effector YopM. Infection and Immunity **80** (ed Bäumler, A. J.) 2519–2527 (2012).

65. Mogensen, T. H. Pathogen Recognition and Inflammatory Signaling in Innate Immune Defenses. Clinical Microbiology Reviews **22,** 240–273 (2009).

66. Mott, H. R. & Owen, D. Structures of Ras superfamily effector complexes: What have we learnt in two decades? Critical Reviews in Biochemistry and Molecular Biology **50,** 85–133 (2015).

67. Mukherjee, S. et al. Yersinia YopJ Acetylates and Inhibits Kinase Activation by Blocking Phosphorylation. Science **312,** 1211–1214 (2006).

68. Müller, P. M. et al. Systems analysis of RhoGEF and RhoGAP regulatory proteins reveals spatially organized RAC1 signalling from integrin adhesions. Nature Cell Biology **22,** 498–511 (2020).

69. Novakovic, B. et al. β-Glucan Reverses the Epigenetic State of LPS-Induced Immunological Tolerance. Cell **167,** 1354–1368.e14 (2016).

70. O'Reilly, D., Quinn, C. M., El-Shanawany, T., Gordon, S. & Greaves, D. R. Multiple Ets Factors and Interferon Regulatory Factor-4 Modulate CD68 Expression in a Cell Type-specific Manner. Journal of Biological Chemistry **278,** 21909–21919 (2003).

71. Ostuni, R. et al. Latent Enhancers Activated by Stimulation in Differentiated Cells. Cell **152,** 157–171 (2013).

72. Pacis, A. et al. Gene activation precedes DNA demethylation in response to infection in human dendritic cells. Proceedings of the National Academy of Sciences **116,** 6938–6943 (2019).

73. Park, S. H. et al. Type I IFNs and TNF cooperatively reprogram the macrophage epigenome to promote inflammatory activation. Nature immunology **18,** 1104 –1116 (2017).

74. Paul, F. et al. Quantitative GTPase Affinity Purification Identifies Rho Family Protein Interaction Partners. Molecular & Cellular Proteomics **16,** 73–85 (2017).

75. Phanstiel, D. H. et al. Static and Dynamic DNA Loops form AP-1-Bound Activation Hubs during Macrophage Development. Molecular Cell **67,** 1037–1048.e6 (2017).

76. Philip, N. H., Zwack, E. E. & Brodsky, I. E. in Inflammasome Signaling and Bacterial Infections 69–90 (Springer International Publishing, Cham, 2016).

77. Quinlan, A. R. & Hall, I. M. BEDTools: a flexible suite of utilities for comparing genomic features. Bioinformatics **26,** 841–842 (2010).

78. Rada-Iglesias, A. et al. A unique chromatin signature uncovers early developmental enhancers in humans. Nature **470,** 279–283 (2011).

79. Reinés, M. et al. Deciphering the Acylation Pattern of Yersinia enterocolitica Lipid A. PLOS Pathogens **8,** 1–21 (2012).

80. Ritchie, M. E. et al. limma powers differential expression analyses for RNA-sequencing and microarray studies. Nucleic Acids Research **43,** e47–e47 (2015).

81. Roach, J. C. et al. Transcription factor expression in lipopolysaccharide-activated peripheral-blood-derived mononuclear cells. Proceedings of the National Academy of Sciences **104,** 16245–16250 (2007).

82. Rolando, M. et al. Legionella pneumophila Effector RomA Uniquely Modifies Host Chromatin to Repress Gene Expression and Promote Intracellular Bacterial Replication. Cell Host & Microbe **13,** 395 –405 (2013).

83. Ruckdeschel, K et al. Interaction of Yersinia enterocolitica with macrophages leads to macrophage cell death through apoptosis. Infection and Immunity **65,** 4813–4821 (1997).

84. Ryan, D. G. & O'Neill, L. A. Krebs Cycle Reborn in Macrophage Immunometabolism. Annual Review of Immunology **38,** 289–313 (2020).

85. Ryu, J. R., Echarri, A., Li, R. & Pendergast, A. M. Regulation of Cell-Cell Adhesion by Abi/Diaphanous Complexes. Molecular and Cellular Biology **29,** 1735–1748 (2009).

86. Saeed, S. et al. Epigenetic programming of monocyte-to-macrophage differentiation and trained innate immunity. Science **345** (2014).

87. Sarhan, J. et al. Caspase-8 induces cleavage of gasdermin D to elicit pyroptosis during Yersinia infection. Proceedings of the National Academy of Sciences **115,** E10888–E10897 (2018).

88. Sauvonnet, N., Pradet-Balade, B., Garcia-Sanz, J. A. & Cornelis, G. R. Regulation of mRNA Expression in Macrophages afterYersinia enterocolitica Infection: ROLE OF DIFFERENT Yop EFFECTORS. Journal of Biological Chemistry **277,** 25133–25142 (2002).

89. Sawicka, A. & Seiser, C. Sensing core histone phosphorylation — A matter of perfect timing. Biochimica et Biophysica Acta (BBA) - Gene Regulatory Mechanisms **1839.** Molecular mechanisms of histone modification function, 711 –718 (2014).

90. Schubert, K. A., Xu, Y., Shao, F. & Auerbuch, V. The Yersinia Type III Secretion System as a Tool for Studying Cytosolic Innate Immune Surveillance. Annual Review of Microbiology **74,**

221–245 (2020).

91. Senoo, H. et al. Phosphorylated Rho-GDP directly activates mTORC2 kinase towards AKT through dimerization with Ras-GTP to regulate cell migration. Nature cell biology **21,** 867—878 (2019).

92. Shen, L. et al. diffReps: Detecting Differential Chromatin Modification Sites from ChIP-seq Data with Biological Replicates. PLOS ONE **8,** 1–13 (2013).

93. Stahnke, S. et al. Loss of Hem1 disrupts macrophage function and impacts migration, phagocytosis, and integrin-mediated adhesion. Current Biology **31,** 2051–2064.e8 (2021).

94. Stiegler, A. L. & Boggon, T. J. The pseudoGTPase group of pseudoenzymes. The FEBS Journal **287,** 4232–4245 (2020).

95. Tajadura-Ortega, V. et al. An RNAi screen of Rho signalling networks identifies RhoH as a regulator of Rac1 in prostate cancer cell migration. BMC Biology **16** (2018).

96. Takeuchi, O. & Akira, S. Pattern Recognition Receptors and Inflammation. Cell **140,** 805 –820 (2010).

97. Tcherkezian, J. & Lamarche-Vane, N. Current knowledge of the large RhoGAP family of proteins. Biology of the Cell **99,** 67–86 (2007).

98. Thorvaldsdóttir, H., Robinson, J. T. & Mesirov, J. P. Integrative Genomics Viewer (IGV): highperformance genomics data visualization and exploration. Briefings in Bioinformatics **14,** 178–192 (2012).

99. Verger, A. & Duterque-Coquillaud, M. When Ets transcription factors meet their partners. BioEssays **24,** 362–370 (2002).

100. Viboud, G. I. & Bliska, J. B. YERSINIA OUTER PROTEINS: Role in Modulation of Host Cell Signaling Responses and Pathogenesis. Annual Review of Microbiology **59,** 69–89 (2005).

101. Vincent, S, Jeanteur, P & Fort, P. Growth-regulated expression of rhoG, a new member of the ras homolog gene family. Molecular and Cellular Biology **12,** 3138–3148 (1992).

102. Wang, Z. et al. Combinatorial patterns of histone acetylations and methylations in the human genome. Nature Genetics **40,** 897–903 (2008).

103. Wennerberg, K. & Der, C. J. Rho-family GTPases: it's not only Rac and Rho (and I like it).

Journal of Cell Science **117,** 1301–1312 (2004).

104. Yamazaki, D., Oikawa, T. & Takenawa, T. Rac-WAVE-mediated actin reorganization is required for organization and maintenance of cell-cell adhesion. Journal of Cell Science **120,** 86–100 (2007).

105. Ye, J. et al. Primer-BLAST: A tool to design target-specific primers for polymerase chain reaction. BMC Bioinformatics **13,** 134 (2012).

106. Yun, M., Workman, J. L. & Li, B. Readers of histone modifications. Cell research **21,** 564–578 (2011).

107. Zang, C. et al. A clustering approach for identification of enriched domains from histone modification ChIP-Seq data. Bioinformatics **25,** 1952–1958 (2009).

108. Zhang, X & Mosser, D. Macrophage activation by endogenous danger signals. The Journal of Pathology **214,** 161–178 (2008).

109. Zhang, Y. et al. Model-based Analysis of ChIP-Seq (MACS). Genome Biology **9,** R137 (2008).

110. Zhou, P. et al. Alpha-kinase 1 is a cytosolic innate immune receptor for bacterial ADP-heptose. Nature **561,** 122–126 (2018).

111. Zipfel, P. A. et al. Role for the Abi/Wave Protein Complex in T Cell Receptor-Mediated Proliferation and Cytoskeletal Remodeling. Current Biology **16,** 35–46 (2006).

Supplementary tables references

1. Abell, A. et al. MAP3K4/CBP-Regulated H2B Acetylation Controls Epithelial-Mesenchymal Transition in Trophoblast Stem Cells. Cell Stem Cell **8,** 525–537 (2011).

2. Biswas, P. S. et al. Phosphorylation of IRF4 by ROCK2 regulates IL-17 and IL-21 production and the development of autoimmunity in mice. The Journal of clinical investigation **120,** 3280—95 (2010).

3. Blank, M. et al. A tumor suppressor function of Smurf2 associated with controlling chromatin landscape and genome stability through RNF20. Nature Medicine **18,** 227–234 (2012).

4. Camps, J., Erdos, M. R. & Ried, T. The role of lamin B1 for the maintenance of nuclear structure and function. Nucleus **6,** 8–14 (2015).

5. Chen, X. et al. Ena/VASP Proteins Cooperate with the WAVE Complex to Regulate the Actin Cytoskeleton. Developmental Cell **30,** 569–584 (2014).

6. Cowell, C. F. et al. Loss of cell–cell contacts induces NF-kB via RhoA-mediated activation of protein kinase D1. Journal of Cellular Biochemistry **106,** 714–728 (2009).

7. Dossin, F. et al. SPEN integrates transcriptional and epigenetic control of X-inactivation. Nature **578,** 455–460 (2020).

8. Du, C. et al. A PRMT5-RNF168-SMURF2 Axis Controls H2AX Proteostasis. Cell Reports **28,** 3199 –3211.e5 (2019).

9. Fazal, F. et al. Essential Role of Cofilin-1 in Regulating Thrombin-induced RelA/p65 Nuclear Translocation and Intercellular Adhesion Molecule 1 (ICAM-1) Expression in Endothelial Cells. Journal of Biological Chemistry **284,** 21047–21056 (2009).

10. Heesemann, J & Laufs, R. Construction of a mobilizable Yersinia enterocolitica virulence plasmid. Journal of Bacteriology **155,** 761–767 (1983).

11. Kang, D. et al. Targeting phospholipase D1 attenuates intestinal tumorigenesis by controlling b-catenin signaling in cancer-initiating cells. The Journal of Experimental Medicine **212,** 1219 –1237 (2015).

12. Kang, D. W. et al. Autoregulation of phospholipase D activity is coupled to selective induction of phospholipase D1 expression to promote invasion of breast cancer cells. International Journal of Cancer **128,** 805–816 (2011).

13. Kang, D. W. et al. Phospholipase D1 Has a Pivotal Role in Interleukin-1b-Driven Chronic Autoimmune Arthritis through Regulation of NF-kB, Hypoxia-Inducible Factor 1a, and FoxO3a. Molecular and Cellular Biology **33,** 2760–2772 (2013).

14. Kang, K. et al. IFN- selectively suppresses a subset of TLR4-activated genes and enhancers to potentiate macrophage activation. Nature Communications **10** (2019).

15. Liao, S., Maertens, O., Cichowski, K. & Elledge, S. J. Genetic modifiers of the BRD4-NUT dependency of NUT midline carcinoma uncovers a synergism between BETis and CDK4/6is. Genes and Development **32,** 1188–1200 (2018).

16. Liu, N. et al. N6-methyladenosine-dependent RNA structural switches regulate RNA–protein

interactions. Nature **518,** 560–564 (2015).

17. Manikoth Ayyathan, D. et al. SMURF2 prevents detrimental changes to chromatin, protecting human dermal fibroblasts from chromosomal instability and tumorigenesis. Oncogene **39,** 3396—3410 (2020).

18. Marinissen, M. J. et al. The Small GTP-Binding Protein RhoA Regulates c-Jun by a ROCK-JNK Signaling Axis. Molecular Cell **14,** 29 –41 (2004).

19. Mathias, R. A., Guise, A. J. & Cristea, I. M. Post-translational Modifications Regulate Class IIa Histone Deacetylase (HDAC) Function in Health and Disease. Molecular & Cellular Proteomics **14,** 456–470 (2015).

20. McNeill, M. C. et al. Nuclear actin regulates cell proliferation and migration via inhibition of SRF and TEAD. Biochimica et Biophysica Acta (BBA) - Molecular Cell Research **1867,** 118691 (2020).

21. Miotto, B. et al. The RBBP6/ZBTB38/MCM10 Axis Regulates DNA Replication and Common Fragile Site Stability. Cell Reports **7,** 575 –587 (2014).

22. Mobley, R. J. et al. MAP3K4 Controls the Chromatin Modifier HDAC6 during Trophoblast Stem Cell Epithelial-to-Mesenchymal Transition. Cell Reports **18,** 2387–2400 (2017).

23. Morgan, M. A. et al. A cryptic Tudor domain links BRWD2/PHIP to COMPASS-mediated histone H3K4 methylation. Genes and Development **31,** 2003–2014 (2017).

24. O'Sullivan, A. G., Mulvaney, E. P., Hyland, P. B. & Kinsella, B. T. Protein kinase C-related kinase

1 and 2 play an essential role in thromboxane-mediated neoplastic responses in prostate cancer. Oncotarget **6,** 26437–26456 (2015).

25. O'Sullivan, A. G., Mulvaney, E. P. & Kinsella, B. T. Regulation of protein kinase C-related kinase (PRK) signalling by the TPa and TPb isoforms of the human thromboxane A2 receptor: Implications for thromboxane- and androgen- dependent neoplastic and epigenetic responses in prostate cancer. Biochimica et Biophysica Acta (BBA) - Molecular Basis of Disease **1863,** 838 –856 (2017).

26. Parsa, S. et al. The serine hydroxymethyltransferase-2 (SHMT2) initiates lymphoma development through epigenetic tumor suppressor silencing. Nature Cancer **1,** 653–664 (2020).

27. Poleshko, A. et al. Human factors and pathways essential for mediating epigenetic gene silencing. Epigenetics **9,** 1280–1289 (2014).

28. Rao, R. A. et al. KMT1 family methyltransferases regulate heterochromatin–nuclear periphery tethering via histone and non-histone protein methylation. EMBO reports **20,** e43260 (2019).

29. Ricker, E. et al. Selective dysregulation of ROCK2 activity promotes aberrant transcriptional networks in ABC diffuse large B-cell lymphoma. Scientific Reports **10,** 13094 (2020).

30. Ricker, E. et al. Serine-threonine kinase ROCK2 regulates germinal center B cell positioning and cholesterol biosynthesis. The Journal of clinical investigation **130,** 3654—3670 (2020).

31. Riento, K. et al. Flotillin proteins recruit sphingosine to membranes and maintain cellular sphingosine-1-phosphate levels. PLOS ONE **13,** 1–18 (2018).

32. Ruckdeschel, K. et al. Yersinia Outer Protein P of Yersinia enterocolitica Simultaneously Blocks the Nuclear Factor-kB Pathway and Exploits Lipopolysaccharide Signaling to Trigger Apoptosis in Macrophages. The Journal of Immunology **166,** 1823–1831 (2001).

33. Sanz-García, M., López-Sánchez, I. & Lazo, P. A. Proteomics Identification of Nuclear Ran GTPase as an Inhibitor of Human VRK1 and VRK2 (Vaccinia-related Kinase) Activities. Molecular & Cellular Proteomics **7,** 2199–2214 (2008).

34. Shendy, N. A. M. et al. Coordinated regulation of Rel expression by MAP3K4, CBP, and HDAC6 controls phenotypic switching. Communications Biology **3,** 475 (2020).

35. Tanaka, T. et al. Nuclear Rho kinase, ROCK2, targets p300 acetyltransferase. The Journal of biological chemistry **281,** 15320—15329 (2006).

36. Toska, E. et al. Repression of Transcription by WT1-BASP1 Requires the Myristoylation of BASP1 and the PIP2-Dependent Recruitment of Histone Deacetylase. Cell Reports **2,** 462–469 (2012).

37. Trülzsch, K., Sporleder, T., Igwe, E. I., Rüssmann, H. & Heesemann, J. Contribution of the Major Secreted Yops of Yersinia enterocolitica O:8 to Pathogenicity in the Mouse Infection Model. Infection and Immunity **72,** 5227–5234 (2004).

38. Vázquez-Cedeira, M., Barcia-Sanjurjo, I., Sanz-García, M., Barcia, R. & Lazo, P. A. Differential Inhibitor Sensitivity between Human Kinases VRK1 and VRK2. PLOS ONE **6,** 1–9 (2011).

39. Weiss, J. M. et al. ROCK2 signaling is required to induce a subset of T follicular helper cells through opposing effects on STATs in autoimmune settings. Science Signaling **9,** ra73–ra73 (2016).

40. Xiao, C. et al. RBBP6, a RING finger-domain E3 ubiquitin ligase, induces epithelial-mesenchymal transition and promotes metastasis of colorectal cancer. Cell Death & Disease **10** (2019).

41. Yu, W. et al. One-Carbon Metabolism Supports S-Adenosylmethionine and Histone Methylation to Drive Inflammatory Macrophages. Molecular Cell **75,** 1147 –1160.e5 (2019).

42. Yu, Y.-L. et al. Smurf2-mediated degradation of EZH2 enhances neuron differentiation and improves functional recovery after ischaemic stroke. EMBO Molecular Medicine **5,** 531–547 (2013).

43. Yun, J. et al. IL-32 gamma reduces lung tumor development through upregulation of TIMP-3 overexpression and hypomethylation. Cell Death & Disease **9** (2018).

44. Zanin-Zhorov, A. et al. Selective oral ROCK2 inhibitor down-regulates IL-21 and IL-17 secretion in human T cells via STAT3-dependent mechanism. Proceedings of the National Academy of Sciences **111,** 16814–16819 (2014).

45. Zheng, X., Kim, Y. & Zheng, Y. Identification of lamin B–regulated chromatin regions based on chromatin landscapes. Molecular Biology of the Cell **26,** 2685–2697 (2015).

Supporting information

Fig S1. Changes of epigenetic histone modifications in *Y. enterocolitica* infected primary human macrophages.

A, Table showing number of detected MACS2 or SICER peaks for each histone mark, fraction of dynamic regions (MACS2 or SICER peaks overlapping significantly (≥ 2-fold

change, adjusted P-value ≤ 0.05) up- or down-regulated diffReps regions) and their distribution at promoters and enhancers.

B, Bar plot showing the total number of unique diffReps regions (differentially enriched regions) for indicated marks altogether identified in the comparisons WAC vs mock, WA314 vs mock and WAC vs WA314.

C, Table showing number of genes associated with differentially enriched regions at promoters or enhancers for comparisons between mock, WAC and WA314. "Total genes up and down" refers to all genes associated with differentially enriched regions at promoters and enhancers when taking all histone marks together for each comparison.

Fig S2. Association between histone modifications at promoters and enhancers and gene expression in *Y. enterocolitica* infected macrophages.

Barplot shows percentage of genes with coordinated promoter and enhancer changes from ChIP-seq profiles overlapping with corresponding RNA-seq profiles.

Fig S3. Pathway and transcription factor enrichment of genes associated with histone modifications whose expression is altered in *Y. enterocolitica* infected macrophages.

A, Heatmap of row-scaled (row Z-score) RNA-seq rlog gene counts belonging to "Inflammatory response" pathway as in Figure 5B.

B, GO terms associated with latent enhancer genes from Figure 4D.

C, Heatmap showing TF motif enrichment in promoter and enhancer regions of genes overlapping in RNA-seq and ChIP-seq as in Figure 5A. Color indicates level of log10 transformed P-value positively correlating with significance of enrichment.

Fig S4. Epigenetic and transcriptional regulation of Rho GTPase pathway genes in *Y. enterocolitica* infected macrophages.

A, Bar plot showing fraction and number (in bars) of indicated Rho GTPase pathway genes with changes in expression only (RNA only), any associated histone modification only (ChIP only), overlaps (RNA & ChIP) and no overlap with neither ChIP-seq nor RNA-seq.

B, Bar plot showing number of Rho GTPase pathway genes with dynamic histone modifications at promoters, enhancers or both (overlap).

C, Table showing number of Rho GTPase pathway genes with histone modification changes at enhancers and number of associated enhancers.

D, E, Heatmaps of DEGs encoding Rho GTPase effectors **(D)** and GEFs **(E)** with associated histone modifications. Associated profiles are color coded on the left. The specificity of GEFs for Rho GTPases is color coded on the right **(E)**. Gene rlog counts were row-scaled (row Z-score).

F, Table showing specificity of Rho GTPase effectors associated with RNA & ChIP overlaps in **(A)** and Figure 6C.

Fig S5. Role of YopM and YopP in the epigenetic and transcriptional reprogramming of macrophages by *Y. enterocolitica*.

A, Principal component analysis of H3K4me3 tag counts in classes P1a-b in 2-4 replicates of macrophages infected with the indicated strains.

B, Percentage YopP effect (median value) for H3K4me3 (P1a-b classes) and H3K27ac (P2a-d, E1-4 classes) when compared to WA314 vs mock (Up and Down profiles) or WA314 vs WAC (Suppression and Prevention profiles)**.**

C, Percentage YopP effect (median value) for DEGs associated with histone modification changes. “Median”: median value when taking % YopP effect from all classes together.

D, Scatter plot of % YopP effect for RNA-seq DEGs and ChIP-seq differential regions associated with Rho GTPase pathway and inflammatory response from Figures 7C, D. Purple dots associated with ABI1 gene are indicated.

E, Western blot analysis of ABI1 levels in primary human macrophages infected with WA314, WA314ΔYopP and WA314ΔYopP+inh (MAPK inhibitors) at an MOI of 100 for 6 h. GAPDH was used as a loading control. Data are representative of two independent experiments.

S1 Table. *Yersinia enterocolitica* strains used in the study.

S2 Table. Analysis of promoter regions. The file contains genomic coordinates, associated genes, normalized counts and percentage YopP effect of regions associated with classes in P1 and P2 promoter modules.

S3 Table. Analysis of enhancer regions. The file contains genomic coordinates, associated genes, normalized counts and percentage YopP effect of regions associated with E1-4 enhancer classes.

S4 Table. Analysis of latent enhancers. The file contains genomic coordinates and associated genes of WAC vs mock latent enhancer regions.

S5 Table. RNA-seq background. The file contains log2 fold change and adjusted P-value for genes from DESeq2 analysis of RNA-seq data.

S6 Table. RNA-seq heatmap. The file contains rlog counts from DESeq2 analysis for DEGs clustered in classes R1-R4.

Table S7. Metabolic pathways in Prevention profile. Analysis was conducted with genes from RNA-seq and ChIP-seq overlaps in Prevention profile. Highlighted pathways include pathways of cholesterol, fatty acids, acyl-CoA or glucose metabolism.

S8 Table. Enriched pathways associated with Rho GTPase pathway genes.

S9 Table. Analysis of Rho GTPase pathway genes in promoter and enhancer classes. The file contains genomic coordinates, normalized counts and activity of Rho GTPase pathway genes from promoter and enhancer classes. H3K4me3 counts are given for P1a-b classes and H3K27ac counts are given for P2a-d and E1-4 classes.

S10 Table. RNA-seq heatmap of Rho GTPase pathway genes. The file contains rlog counts from DESeq2 analysis and activity of Rho GTPase pathway genes associated with RNA-seq classes R1-4.

S11 Table. Rho GTPase specificity of GAPs and GEFs with RNA-seq and ChIP-seq overlaps in different profiles.

S12 Table. Rho GTPase specificity and reported function in epigenetics for effectors with RNA-seq and ChIP-seq overlaps.

S13 Table. Analysis of YopP effect on Rho GTPase pathway genes. The file contains % YopP effect on epigenetic and gene expression changes of genes from Rho GTPase pathway in Suppression and Prevention profiles. Genes, associated regions with histone mark changes and % YopP effect are indicated. Only genes with significant WAC vs WA314 RNA-seq and ChIP-seq change were analysed. "Average" indicates average % YopP effect on ChIP-seq regions and RNA-seq genes (unique).

S14 Table. Analysis of YopP effect on inflammatory response pathway genes. The file contains % YopP effect on epigenetic and gene expression changes of genes from inflammatory response pathway in Suppression profile. Genes, associated regions with histone mark changes and % YopP effect are indicated. Only genes with significant WAC vs WA314 RNA-seq and ChIP-seq change were analysed. "Average" indicates average % YopP effect on ChIP-seq regions and RNA-seq genes (unique).

S15 Table. Primer sequences used for ChIP-qPCR for differential enrichment analysis.

Figure Captions

Fig 1. Changes of epigenetic histone modifications in *Y. enterocolitica* infected primary human macrophages.

A, Experimental design. $CD14^{+}$ monocytes were isolated and differentiated into macrophages by cultivation with 20 % human serum for 6 days. Macrophages from ≥ two independent donors were mock infected or infected with avirulent *Y. enterocolitica* strain WAC, wild type strain WA314 or the single Yop-mutant strains WA314ΔYopM and WA314ΔYopP for 6 h. Samples were subjected to ChIP-seq for histone modifications H3K27ac, H3K4me3 and RNA-seq. H3K4me1 and H3K27me3 ChIP-seq was performed only for mock, WAC and WA314 infected macrophages.

B, Bar plot showing proportions of dynamic and constant regions of ChIP-seq data obtained from mock-, WAC- and WA314 infected macrophages as described in **(A)**. Dynamic regions were defined as MACS (H3K4me3, H3K27ac) or SICER (H3K4me1, H3K27me3) peaks overlapping significantly (≥ 2-fold change, adjusted P-value ≤ 0.05) up- or down-regulated diffReps regions in the three pairwise comparisons WAC vs mock, WA314 vs mock and WAC vs WA314.

C, Bar plot showing distribution of dynamic regions from **(B)** at gene promoters and enhancers.

D, Heatmap showing Spearman correlation (cor.) of H3K27ac tag density at all H3K27ac peaks from mock-, WAC- and WA314-infected samples and publicly available H3K27ac ChIP-seq data of naive* and LPS* treated macrophages. Low to high correlation is indicated by blue-white-red colour scale.

E, Number of differentially enriched regions (diffReps ≥ 2-fold change, adjusted P-value ≤ 0.05) for the indicated histone marks.

F, G, Venn diagrams of differentially enriched region overlaps showing suppression of WAC induced upregulation of H3K4me3 marks by WA314 **(F)** and suppression of WAC induced up-regulation of H3K27ac marks by WA314 or prevention of WAC induced down-regulation of H3K27ac marks by WA314 **(G)**.

H, Bar plot showing the number of genes associated with promoters, enhancers or both in total or for the indicated histone marks associated with dynamic regions in **(E)**.

Fig 2. Dynamic H3K4me3 and H3K27ac modifications at promoters in *Y. enterocolitica* infected macrophages.

A, Heatmap showing clustering of H3K4me3 (module P1) and H3K27ac (module P2) differential regions at promoters in mock-, WAC- and WA314 infected human macrophages. P1 contains dynamic H3K4me3- and H3K27ac regions that change concordantly and P2 contains dynamic H3K27ac regions at largely constant H3K4me3 regions. H3K4me3 and H3K27ac tag densities are shown in both modules. The identified clusters (colour coded bars on the left side) were grouped in classes P1a-P2d. Rows are genomic regions from -10 to +10 kb around the centre of the analyzed regions. n indicates number of regions in the respective classes.

B, Boxplots of H3K4me3 and H3K27ac tag counts for the classes in **(A)**. Profiles describing relation of histone mark levels between mock, WAC and WA314 are indicated on top. Data are representative of at least two independent experiments.

C, D Peak tracks of H3K4me3 (red) and H3K27ac (blue) tag densities at promoter regions of the genes OASL from Suppression profile classes P1a and ACOT7 from Prevention profile class P1b **(C)** and ZNF513 from Down profile class P2b and SLC30A3 from Up profile class P2c **(D)**.

E, Schematic summarizing *Yersinia* counter-regulation of PAMP-induced H3K4me3 and H3K27ac changes at promoters. Arc arrows indicate deposition or removal of histone marks, whose levels are signified by different size.

Fig 3. H3K4me1 and dynamic H3K27ac modifications at distal regulatory elements/enhancers in *Y. enterocolitica* infected macrophages.

A, Heatmap showing clustering of H3K27ac differential regions at enhancers of mock-, WAC- and WA314 infected macrophages. H3K4me1 tag counts are shown for the associated regions. Clustering analysis yielded 6 clusters (color coded, left side) which were assembled into classes E1-4. Rows are genomic regions from -10 to +10 kb around the centre of the analyzed regions. n indicates number of regions

B, Boxplot of H3K27ac tag counts of classes E1-E4 in **(A)**. Profiles describing relation of histone mark levels between mock, WAC and WA314 are indicated on top. Data are representative of two independent experiments.

C, Peak tracks of H3K4me3- (red), H3K27ac- (blue) and H3K4me1 (green) tag densities at promoter (orange box) and enhancer (purple box) regions of Suppression profile gene IL1A. Data are suggestive of coordinative regulation of H3K4me3 and H3K27ac at the promoter and H3K27ac at an enhancer of the IL1A gene (see also corresponding gene expression data of IL1A in S5 Table).

D, Heatmap showing H3K4me1 and H3K27ac tag counts at latent enhancers induced by WAC vs mock. Rows are genomic regions from -10 to +10 kb around the centre of the analyzed regions. n indicates number of regions.

Fig 4. Association between histone modifications at promoters and enhancers and gene expression in *Y. enterocolitica* infected macrophages.

A, Heatmap from clustering of all DEGs from mock, WAC and WA314 comparisons. Clustering identified 4 major classes R1-R4 (color coded, right side). Profiles describing relation of expression levels between mock, WAC and WA314 are indicated on the left. In the heatmap, gene rlog counts are row-scaled (row Z-score).

B, C, Venn diagrams of DEG overlaps between WAC vs mock up and WAC vs WA314 up **(B)** and WAC vs mock down and WAC vs WA314 down **(C)**. Overlaps show the number of genes whose up-regulation by WAC is suppressed by WA314 **(B)** and whose down-regulation by WAC is prevented by WA314 **(C)**.

D-G, Bar plots showing fraction (%) of genes associated with H3K4me3 at promoters **(D)**, H3K27ac at promoters **(E)**, H3K4me3 and H3K27ac at promoters **(F)** and H3K27ac at enhancers **(G)** showing respective changes in gene expression (≥ 2-fold change, adjusted P-value ≤ 0.05).

H, Barplot showing percentage of genes from ChIP-seq profiles overlapping with corresponding RNA-seq profiles.

I, Heatmap presentation showing relative overlap of genes in promoter classes P1a-P2d and enhancer classes E1-4. Light to dark color scale indicates low to high overlap.

J, Schematic summarizing *Yersinia's* coordinated counter-regulation of PAMP-induced H3K4me3 and H3K27ac changes at promoters and enhancers. Levels of color-coded histone marks are signified by their size. Size of TSS arrows and number of transcripts indicate transcriptional activity.

Fig 5. Pathway and transcription factor enrichment of genes associated with histone modifications whose expression is altered in *Y. enterocolitica* infected macrophages.

A, Bar plot showing fraction and number (numbers in bars) of genes from RNA-seq profiles overlapping with corresponding ChIP-seq profiles.

B, Bar plot showing enriched GO and KEGG (hsa prefix) terms for genes overlapping in RNA-seq and ChIP-seq as in **(A)**. Bars represent log10 transformed P-values correlating with significance of enrichment. Pos: positive, reg: regulation, pol: polymerase, prom: promoter.

C-E, Heatmaps of row-scaled (row Z-score) RNA-seq rlog gene counts for genes from pathways in **(B)**.

F, Representative enriched transcription factor motifs in promoter and enhancer regions of genes overlapping in RNA-seq and ChIP-seq as in **(A)**.

Fig 6. Epigenetic and transcriptional regulation of Rho GTPase pathway genes in *Y. enterocolitica* infected macrophages.

A, Number of Rho GTPase pathway genes associated with regions in promoter and enhancer classes including number of total unique genes and regions.

B, Heatmap of all DEGs from Rho GTPase pathway in classes R1-R4 (color coded, right side) and their correlation with profiles (left side). n refers to the number of genes. Gene rlog counts were row-scaled (row Z-score).

C, Bar plot showing fraction and number of genes from RNA-seq profiles in **(B)** overlapping with corresponding promoter and/ or enhancer regions from the same profiles.

D, Bar plot showing specificities of active GAPs (Müller et al., 2020) from overlaps in **(C)** for Rac1, RhoA and multiple Rho GTPases. Fraction and number (in bars) for all identified GAPs and for GAPs in the Suppression and Prevention profiles are shown.

E, F, Heatmaps of GAP **(E)** and Rho GTPase genes **(F)** from overlaps in **(C)**. Associated profiles are indicated on the left and specificity of GAPs for Rho GTPases are indicated on the right. Gene rlog counts were row-scaled (row Z-score).

G,Table showing DEGs (from Fig 4A, S6 Table) known to regulate ubiquitination and/ or proteosomal degradation of Rho GTPases.

H, Schematic representation of Rho GTPase cycle and reprogrammed Rho GTPase pathway genes divided into GAPs, GEFs, Rho GTPases and effectors, and assigned to profiles.

Fig 7. Role of YopP and YopM in the epigenetic and transcriptional reprogramming of macrophages by *Y. enterocolitica*.

A, Principal component analysis of H3K27ac tag counts in classes P1a-P2d and E1-4 in two replicates of macrophages infected with the indicated strains.

B, Number of DEGs (≥ 2-fold change, adjusted P-value ≤ 0.05) and differential H3K4me3 and H3K27ac regions (≥ 2-fold change, adjusted P-value ≤ 0.05) for WA314ΔYopM vs WA314 and WA314ΔYopP vs WA314.

C, D, Percentage of WA314 effect on expression of Rho GTPase pathway genes **(C)** or genes of the inflammatory response **(D)** associated with histone modifications that is caused by YopP. The percentage value was calculated from the ratio of fold change (FC) between WA314ΔYopP vs WA314 and WA314 vs WAC for Suppression **(C, D)** and Prevention **(C)** profiles.

E, Peak tracks of tag densities showing H3K4me3 and H3K27ac changes associated with IL2RA gene, whose suppression of gene expression by WA314 is produced in a YopP-dependent manner **(D)**. H3K4me3 and H3K27ac densities at the IL2RA promoter (orange box) and H3K27ac densities at the enhancers (purple boxes) are not affected by YopP (compare effects of WA314 and WA314ΔYopP).

F, H3K4me3 and H3K27ac ChIP-qPCR signals at indicated genes in macrophages not infected (mock) or infected with indicated strains. WA314ΔYopP infections occurred in the absence and presence of MAPK inhibitors (inh). The ChIP-qPCR signal was expressed as relative (rel.) enrichment (enr.) vs mock. Lines represent mean of 3 biological replicates (dots with different shapes). SOCS3: Suppressor of cytokine signaling 3, IDO1: Indoleamine 2,3-Dioxygenase 1, PTGS2: Prostaglandin-Endoperoxide Synthase 2.

G, Immunofluorescence staining of primary human macrophages infected with WA314, WA314ΔYopP+inh (MAPK inhibitors) and WA314ΔYopP at an MOI of 100 for 6 h. Cells were stained with Alexa568 phalloidin (red) to visualize actin and antibodies for ABI1 (cyan), vinculin (blue) and ZO-1 (green). Fourth column shows overlay of actin and ABI1 (top) and actin, vinculin and ZO-1 (bottom) for WA314ΔYopP infection. Data are representative of two independent experiments.

H, Quantification of actin (left) and ABI1 (right) signal intensity at cell junctions from immunofluorescence of primary human macrophages infected with WA314, WA314ΔYopP+inh (MAPK inhibitors) and WA314ΔYopP at an MOI of 100 for 6 h. Bars show mean and error bars represent standard deviation. ****: P-adjusted < 0.0001 by unpaired Wilcoxon test. Data are representative of two independent experiments.

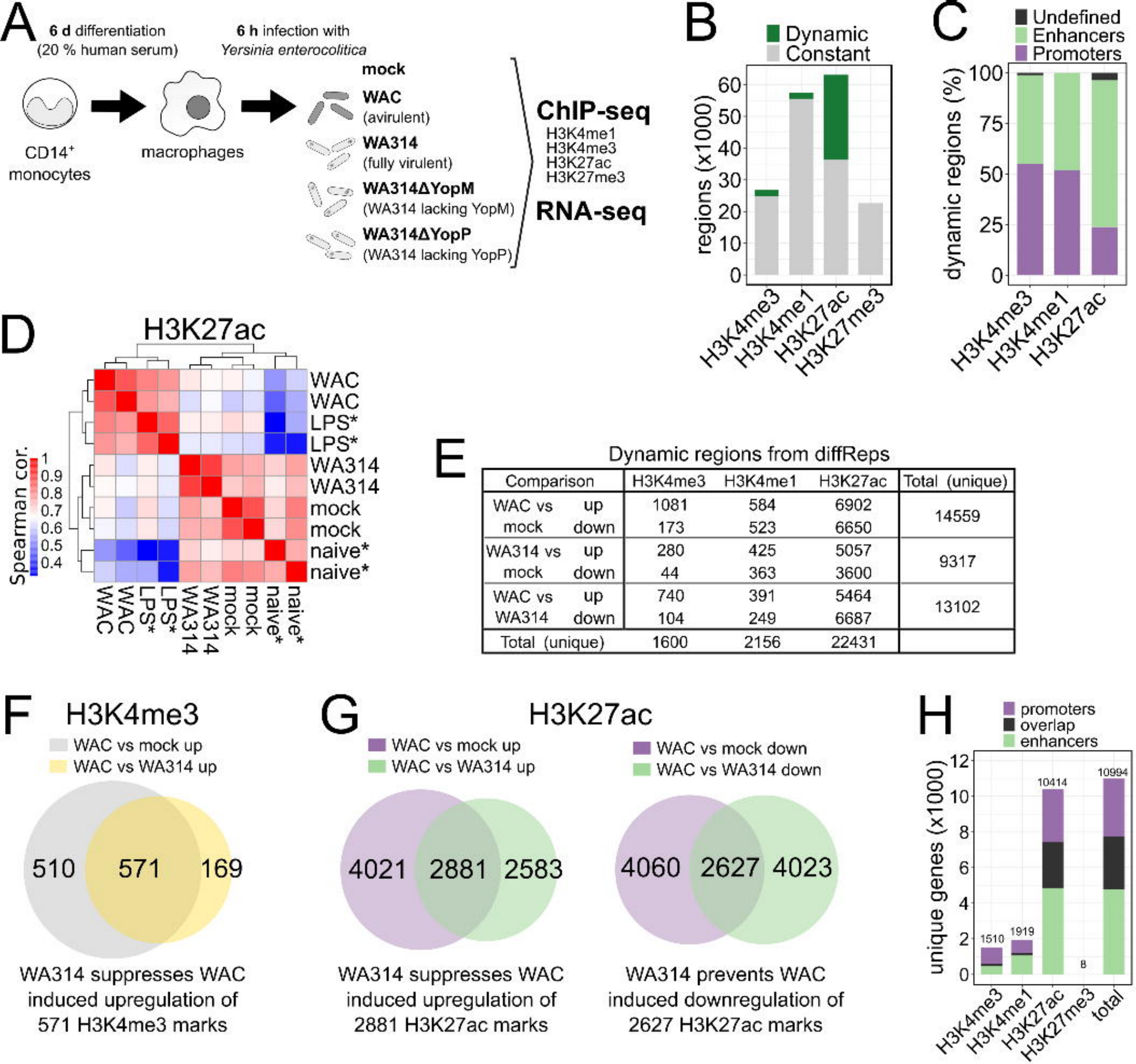

Comparison		H3K4me3	H3K4me1	H3K27ac	Total (unique)
WAC vs mock	up	1081	584	6902	14559
	down	173	523	6650	
WA314 vs mock	up	280	425	5057	9317
	down	44	363	3600	
WAC vs WA314	up	740	391	5464	13102
	down	104	249	6687	
Total (unique)		1600	2156	22431	

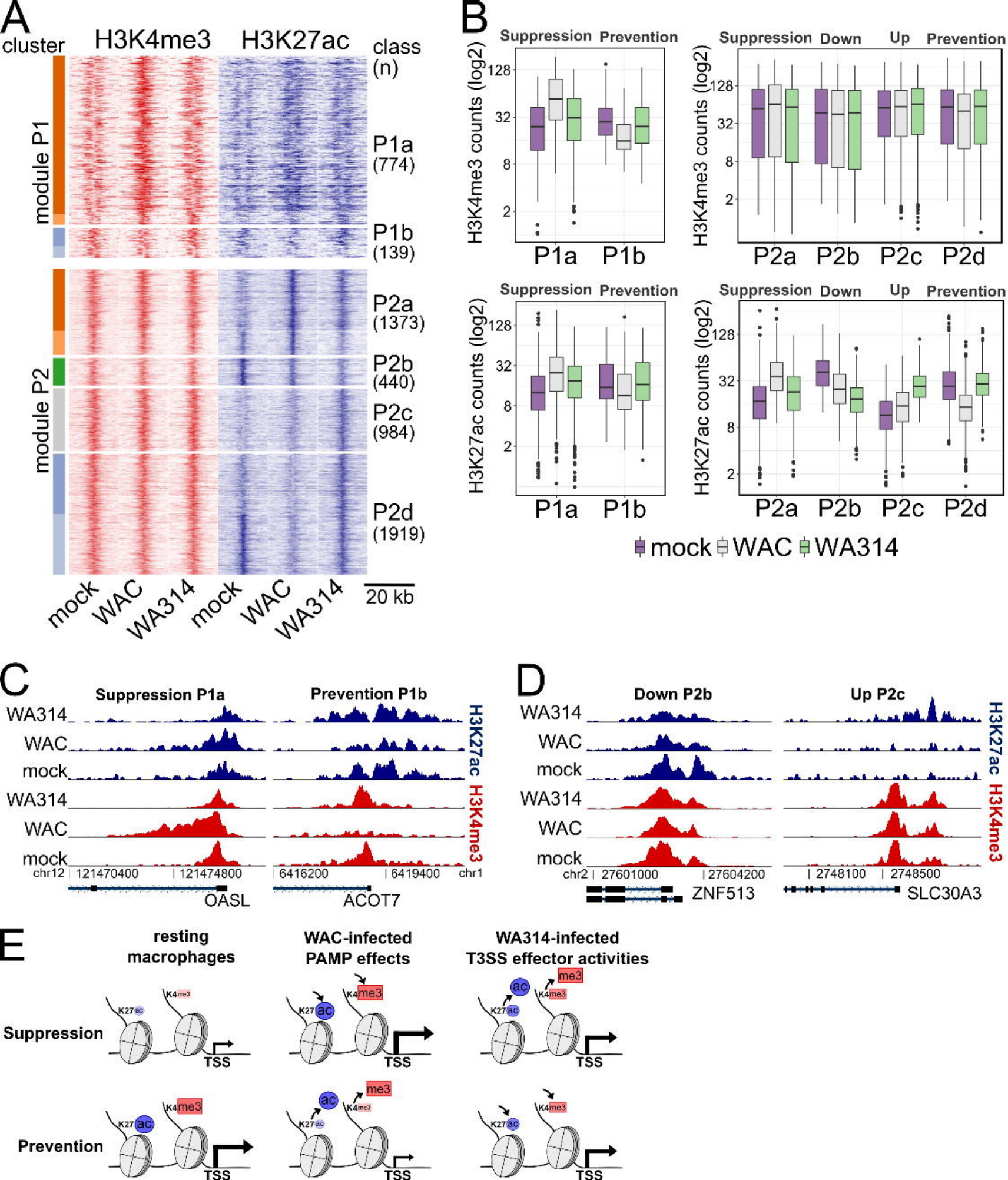
A
cluster
H3K4me3
H3K27ac
class (n)
module P1
P1a (774)
P1b (139)
module P2
P2a (1373)
P2b (440)
P2c (984)
P2d (1919)
mock
WAC
WA314
mock
WAC
WA314
20 kb
B
Suppression
Prevention
H3K4me3 counts (log2)
P1a
P1b
Suppression
Down
Up
Prevention
H3K4me3 counts (log2)
P2a
P2b
P2c
P2d
H3K27ac counts (log2)
H3K27ac counts (log2)
mock
WAC
WA314
C
Suppression P1a
Prevention P1b
WA314
WAC
mock
WA314
WAC
mock
H3K27ac
H3K4me3
chr12
121470400
121474800
6416200
6419400
chr1
OASL
ACOT7
D
Down P2b
Up P2c
WA314
WAC
mock
WA314
WAC
mock
H3K27ac
H3K4me3
chr2
27601000
27604200
2748100
2748500
ZNF513
SLC30A3
E
resting macrophages
WAC-infected PAMP effects
WA314-infected T3SS effector activities
Suppression
Prevention
K27ac
K4me3
TSS

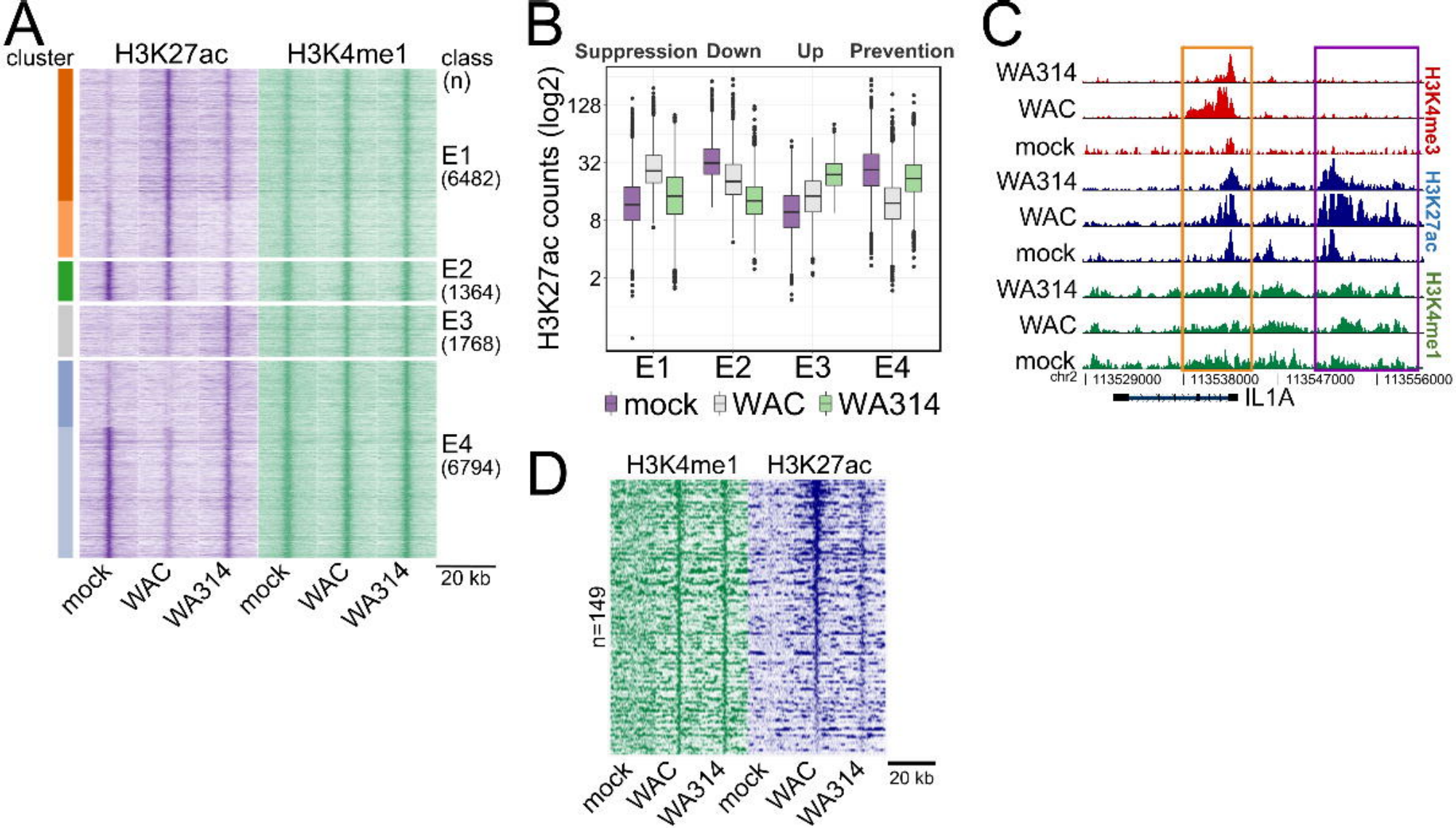
A
cluster
H3K27ac
H3K4me1
class (n)
E1 (6482)
E2 (1364)
E3 (1768)
E4 (6794)
mock
WAC
WA314
mock
WAC
WA314
20 kb
B
Suppression
Down
Up
Prevention
H3K27ac counts (log2)
128
32
8
2
E1
E2
E3
E4
mock
WAC
WA314
C
WA314
WAC
mock
WA314
WAC
mock
WA314
WAC
mock
H3K4me3
H3K27ac
H3K4me1
chr2
113529000
113538000
113547000
113556000
IL1A
D
H3K4me1
H3K27ac
n=149
mock
WAC
WA314
mock
WAC
WA314
20 kb

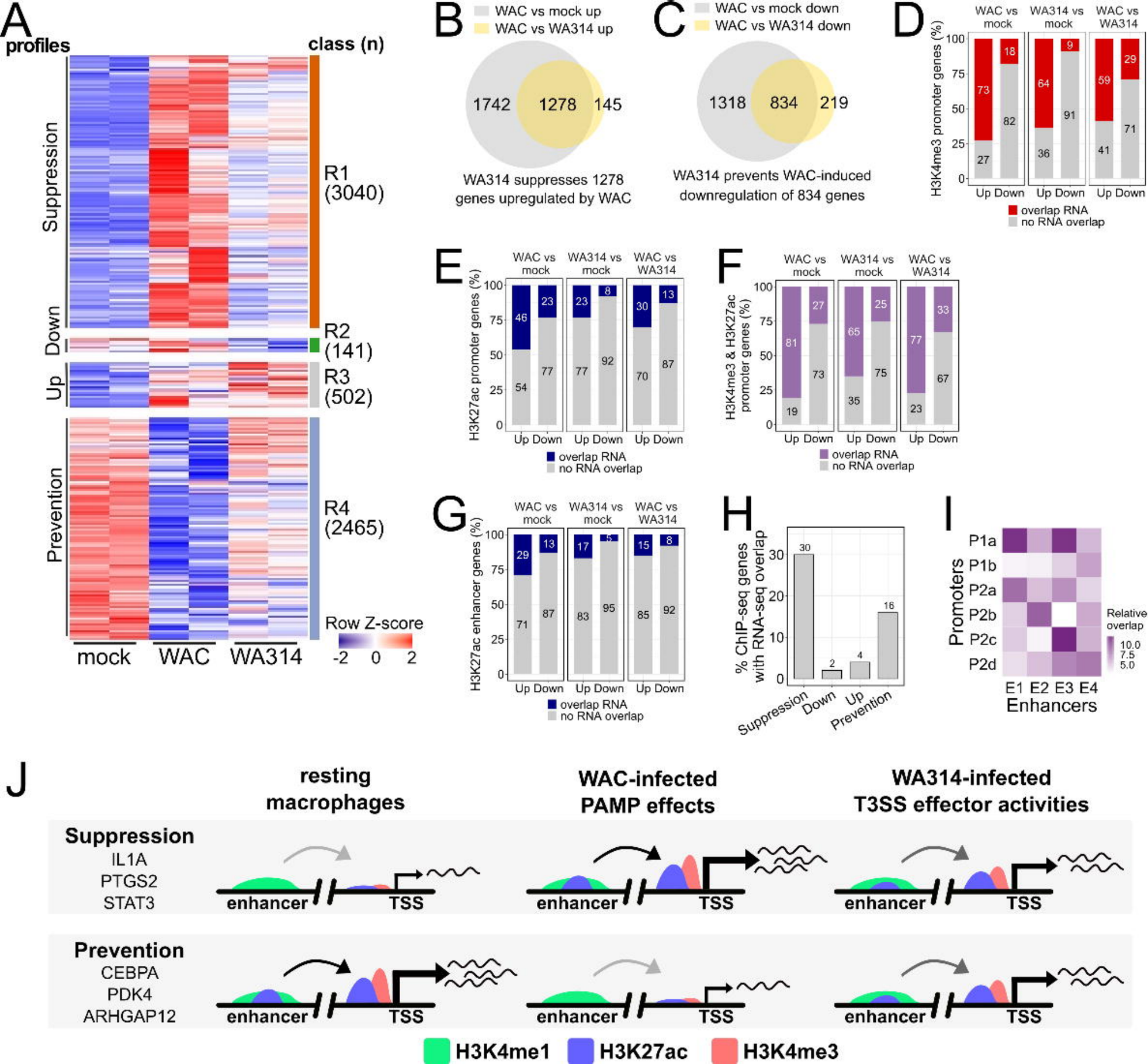
A
profiles
class (n)
Suppression
Down
Up
Prevention
R1 (3040)
R2 (141)
R3 (502)
R4 (2465)
Row Z-score
-2 0 2
mock
WAC
WA314
B
WAC vs mock up
WAC vs WA314 up
1742 1278 145
WA314 suppresses 1278 genes upregulated by WAC
C
WAC vs mock down
WAC vs WA314 down
1318 834 219
WA314 prevents WAC-induced downregulation of 834 genes
D
WAC vs mock
WA314 vs mock
WAC vs WA314
H3K4me3 promoter genes (%)
overlap RNA
no RNA overlap
E
H3K27ac promoter genes (%)
F
H3K4me3 & H3K27ac promoter genes (%)
G
H3K27ac enhancer genes (%)
H
% ChIP-seq genes with RNA-seq overlap
Suppression
Down
Up
Prevention
I
Promoters
P1a
P1b
P2a
P2b
P2c
P2d
E1 E2 E3 E4
Enhancers
Relative overlap
J
resting macrophages
WAC-infected PAMP effects
WA314-infected T3SS effector activities
Suppression
IL1A
PTGS2
STAT3
Prevention
CEBPA
PDK4
ARHGAP12
enhancer
TSS
H3K4me1
H3K27ac
H3K4me3

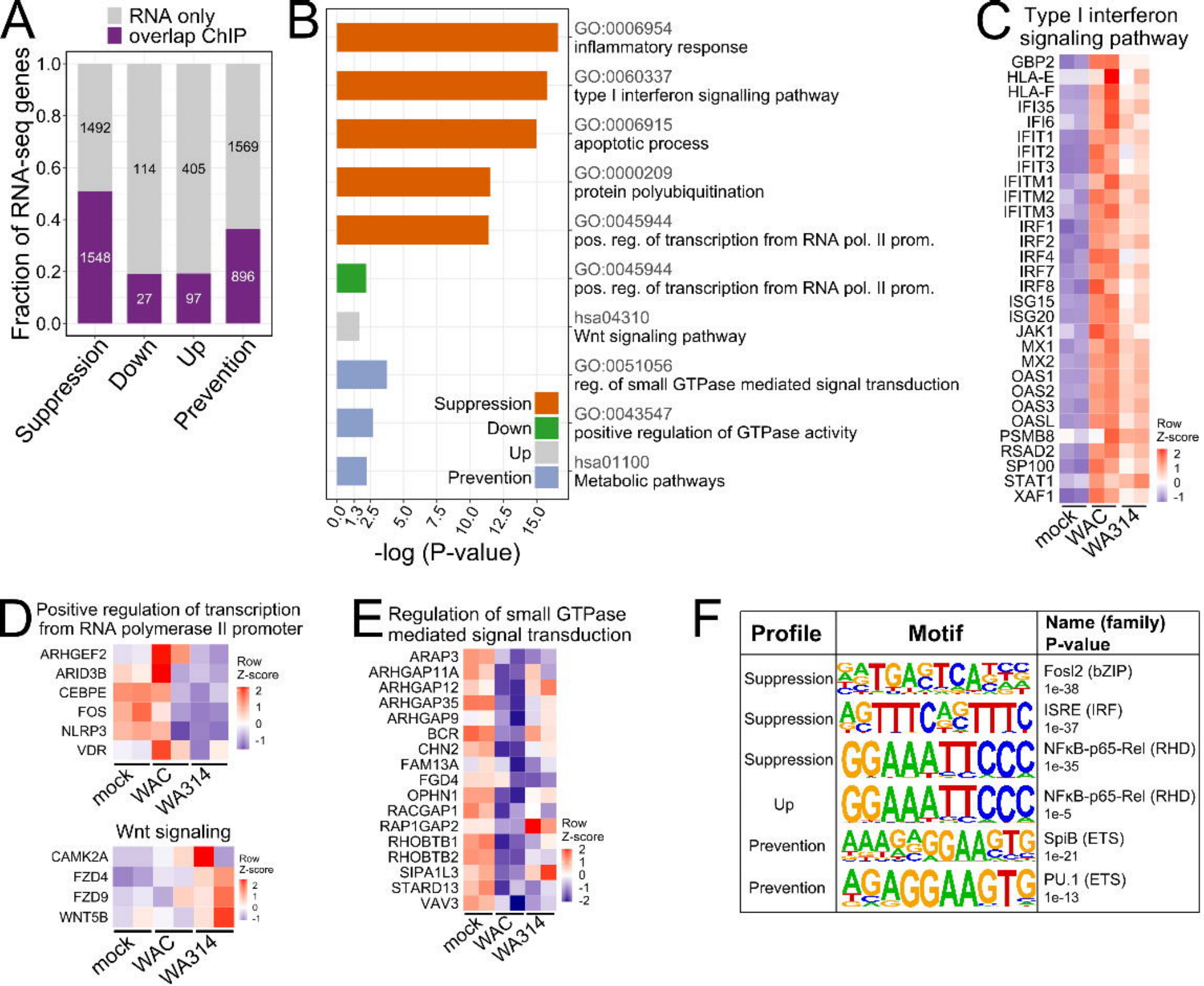
A
RNA only
overlap ChIP
Fraction of RNA-seq genes
1.0
0.8
0.6
0.4
0.2
0.0
1492
1548
114
27
405
97
1569
896
Suppression
Down
Up
Prevention
B
GO:0006954
inflammatory response
GO:0060337
type I interferon signalling pathway
GO:0006915
apoptotic process
GO:0000209
protein polyubiquitination
GO:0045944
pos. reg. of transcription from RNA pol. II prom.
GO:0045944
pos. reg. of transcription from RNA pol. II prom.
hsa04310
Wnt signaling pathway
GO:0051056
reg. of small GTPase mediated signal transduction
GO:0043547
positive regulation of GTPase activity
hsa01100
Metabolic pathways
Suppression
Down
Up
Prevention
0.0
1.3
2.5
5.0
7.5
10.0
12.5
15.0
-log (P-value)
C
Type I interferon signaling pathway
GBP2
HLA-E
HLA-F
IFI35
IFI6
IFIT1
IFIT2
IFIT3
IFITM1
IFITM2
IFITM3
IRF1
IRF2
IRF4
IRF7
IRF8
ISG15
ISG20
JAK1
MX1
MX2
OAS1
OAS2
OAS3
OASL
PSMB8
RSAD2
SP100
STAT1
XAF1
Row Z-score
2
1
0
-1
mock
WAC
WA314
D
Positive regulation of transcription from RNA polymerase II promoter
ARHGEF2
ARID3B
CEBPE
FOS
NLRP3
VDR
Row Z-score
2
1
0
-1
mock
WAC
WA314
Wnt signaling
CAMK2A
FZD4
FZD9
WNT5B
Row Z-score
2
1
0
-1
mock
WAC
WA314
E
Regulation of small GTPase mediated signal transduction
ARAP3
ARHGAP11A
ARHGAP12
ARHGAP35
ARHGAP9
BCR
CHN2
FAM13A
FGD4
OPHN1
RACGAP1
RAP1GAP2
RHOBTB1
RHOBTB2
SIPA1L3
STARD13
VAV3
Row Z-score
2
1
0
-1
-2
mock
WAC
WA314
F
Profile
Motif
Name (family)
P-value
Suppression
Fosl2 (bZIP)
1e-38
Suppression
ISRE (IRF)
1e-37
Suppression
NFκB-p65-Rel (RHD)
1e-35
Up
NFκB-p65-Rel (RHD)
1e-5
Prevention
SpiB (ETS)
1e-21
Prevention
PU.1 (ETS)
1e-13

A

Altered genes and regions from Rho GTPase pathway

Profile	Class	Genes	Regions
Suppression	P1a	34	36
	P2a	55	59
	E1	152	338
Down	P2b	7	7
	E2	46	56
Up	P2c	56	61
	E3	66	88
Prevention	P1b	3	3
	P2d	77	88
	E4	141	287
	unique	**324**	**1023**

B

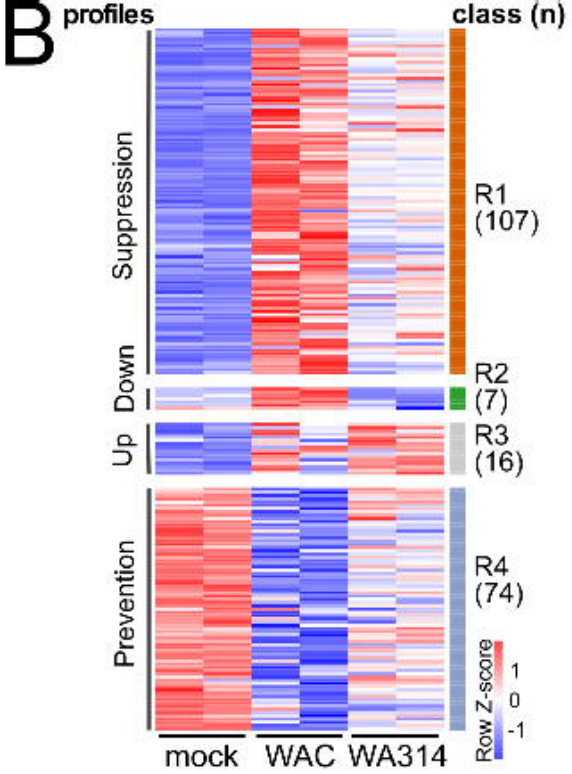

C

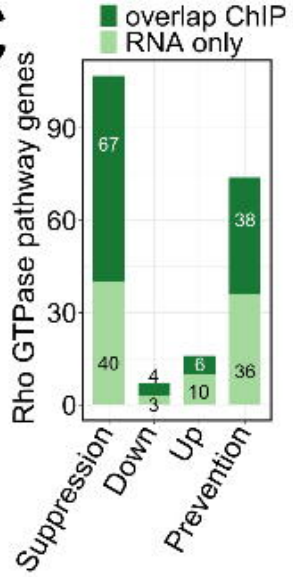

D

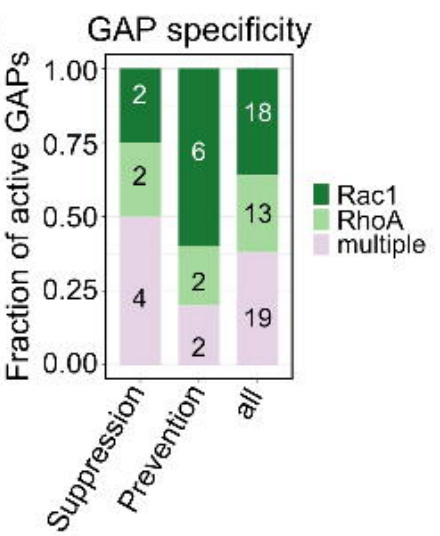

E

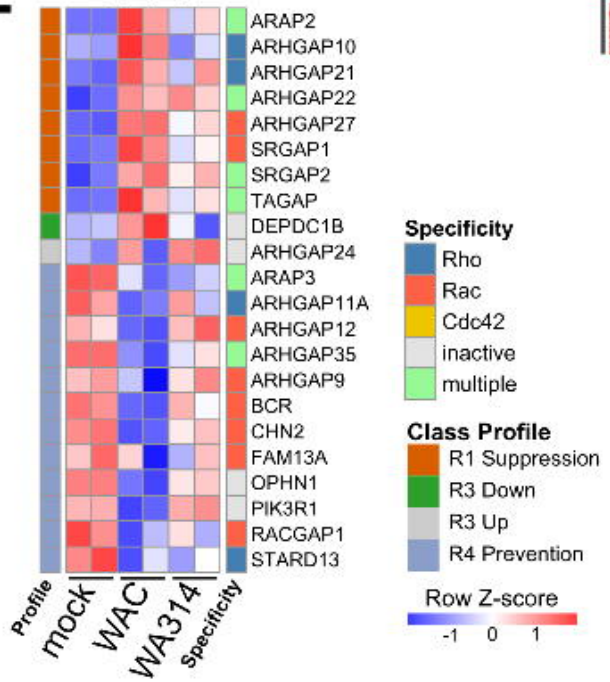

F

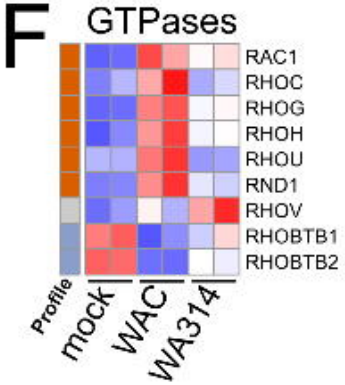

G

DEGs involved in Rho GTPase ubiquitination and/ or degradation

SYMBOL (*associated epigenetic change)	Profile	Function
XIAP*	Suppression	Rac1 polyubiquitination for degradation
BIRC2 (cIAP1)*	Suppression	
SMURF1*	Suppression	RhoA and RhoB proteosomal degradation
TNFAIP1 (BACURD2)*	Suppression	RhoA GDP proteosomal degradation
FBXW7	Suppression	RhoA proteosomal degradation
SKP2	Prevention	Rnd3 degradation in cell cycle control

H

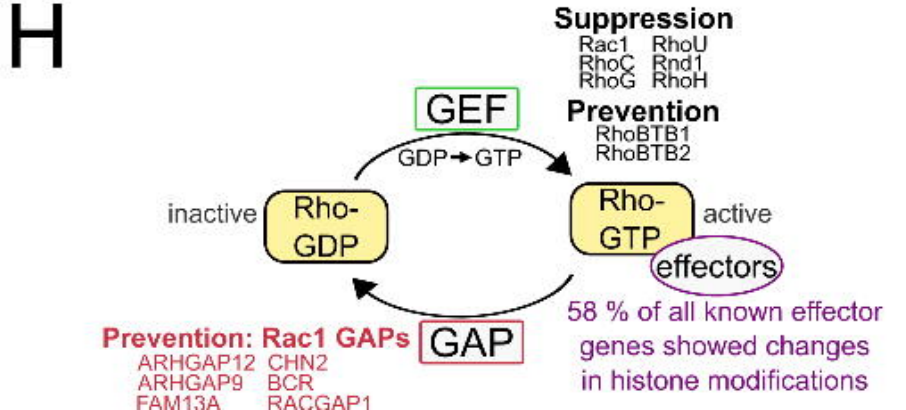

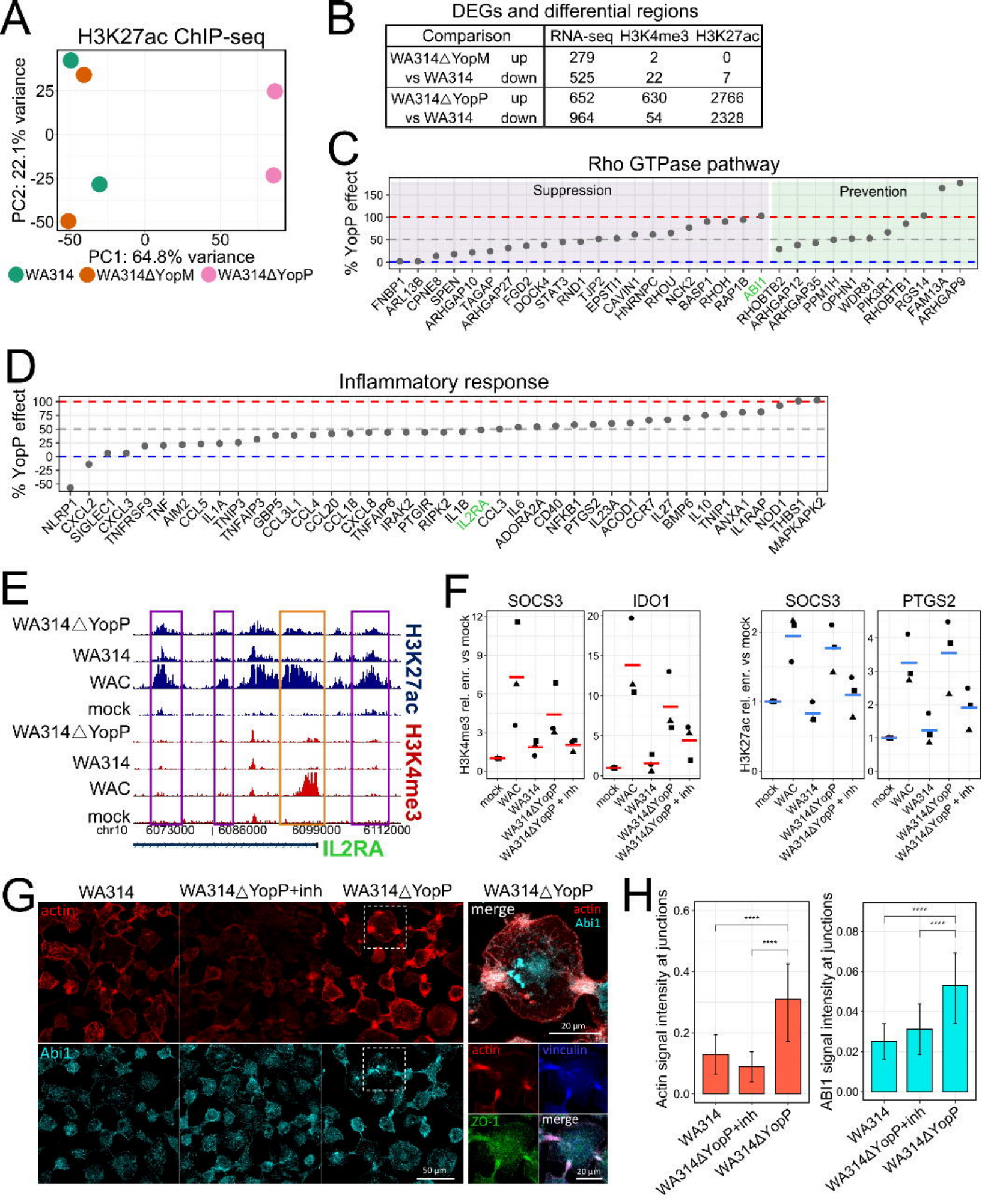
A
H3K27ac ChIP-seq
PC2: 22.1% variance
PC1: 64.8% variance
WA314
WA314ΔYopM
WA314ΔYopP
B
DEGs and differential regions
Comparison
RNA-seq
H3K4me3
H3K27ac
WA314ΔYopM vs WA314 up 279 2 0
WA314ΔYopM vs WA314 down 525 22 7
WA314ΔYopP vs WA314 up 652 630 2766
WA314ΔYopP vs WA314 down 964 54 2328
C
Rho GTPase pathway
% YopP effect
Suppression
Prevention
FNBP1 ARL13B CPNE8 SPEN ARHGAP10 TAGAP ARHGAP27 FGD2 DOCK4 STAT3 RND1 TJP2 EPSTI1 CAVIN1 HNRNPC RHOU NCK2 BASP1 RHOH RAP1B ABI1 RHOBTB2 ARHGAP12 ARHGAP35 PPM1H OPHN1 WDR81 PIK3R1 RHOBTB1 RGS14 FAM13A ARHGAP9
D
Inflammatory response
% YopP effect
NLRP1 CXCL2 SIGLEC1 CXCL3 TNFRSF9 TNF AIM2 CCL5 IL1A TNIP3 TNFAIP3 GBP5 CCL3L1 CCL4 CCL20 CCL18 CXCL8 TNFAIP6 IRAK2 PTGIR RIPK2 IL1B IL2RA CCL3 IL6 ADORA2A CD40 NFKB1 PTGS2 IL23A ACOD1 CCR7 IL27 BMP6 IL10 TNIP1 ANXA1 IL1RAP NOD1 THBS1 MAPKAPK2
E
WA314△YopP
WA314
WAC
mock
H3K27ac
H3K4me3
chr10 6073000 6086000 6099000 6112000
IL2RA
F
SOCS3
IDO1
SOCS3
PTGS2
H3K4me3 rel. enr. vs mock
H3K27ac rel. enr. vs mock
mock
WAC
WA314
WA314ΔYopP
WA314ΔYopP + inh
G
WA314
WA314△YopP+inh
WA314△YopP
WA314△YopP
actin
Abi1
merge
actin
Abi1
20 μm
actin
vinculin
ZO-1
merge
20 μm
50 μm
H
Actin signal intensity at junctions
ABI1 signal intensity at junctions
****
WA314
WA314ΔYopP+inh
WA314ΔYopP

A

Identified peaks and fraction of dynamic peaks

Histone mark (peak caller)	Peaks or regions			% dynamic peaks or regions		
	Total	Dynamic	% dynamic	Promoters	Enhancers	Undefined
H3K4me3 (MACS2)	26791	1939	7.2	55.1	43.8	1.1
H3K4me1 (SICER)	57519	1984	3.4	51.8	48.2	0.0
H3K27ac (MACS2)	63120	26819	42.5	23.8	72.5	3.7
H3K27me3 (SICER)	22645	12	0.1	50.0	33.3	16.7

B

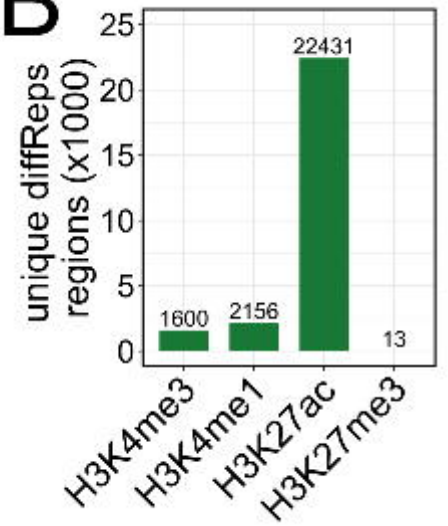

C

Associated genes

Comparison		H3K4me3		H3K27me3		H3K4me1		H3K27ac		total genes up and down (unique)
		promoters	enhancers	promoters	enhancers	promoters	enhancers	promoters	enhancers	
WAC vs mock	up	726	351	0	0	179	372	1594	2958	7745
	down	87	97	1	1	217	307	1507	3195	
WA314 vs mock	up	171	108	0	0	33	358	1692	2249	5900
	down	34	13	0	1	186	193	640	2051	
WAC vs WA314	up	457	283	0	0	394	80	920	2749	7550
	down	52	60	5	1	46	197	2106	2854	

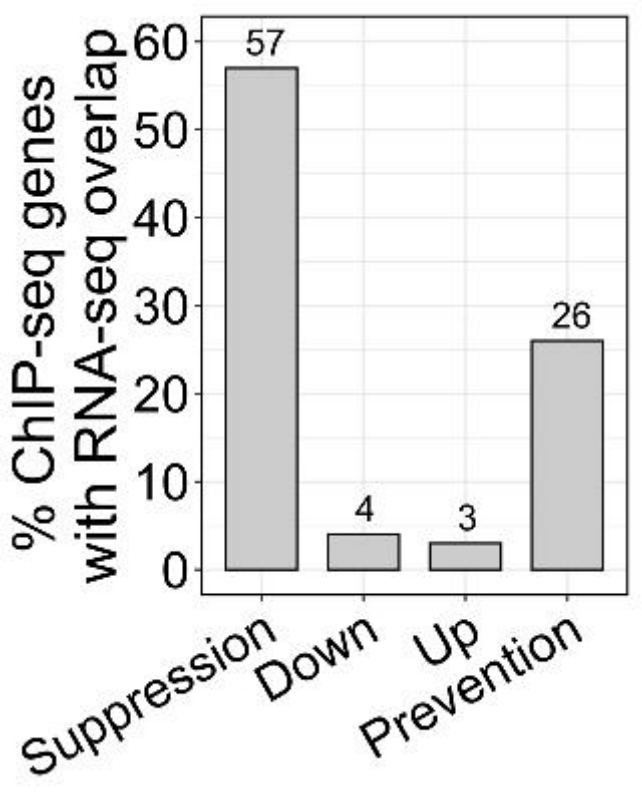
% ChIP-seq genes with RNA-seq overlap
0
10
20
30
40
50
60
57
4
3
26
Suppression
Down
Up
Prevention

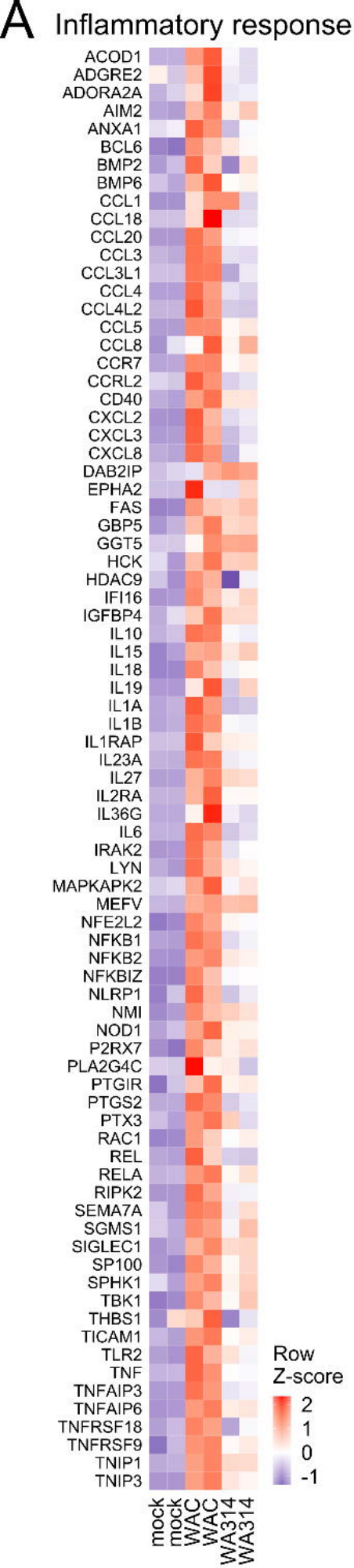

B

GO terms associated with latent enhancers

Term	P-value	Genes
GO:0000122~negative regulation of transcription from RNA polymerase II promoter	1.13E-04	ATF7IP, SP100, EDN1, BCL11A, NEDD4L, RBPJ, NFKB1, FOXP1, ZEB2, REST, H2AFY2, REL, PKIG, JARID2, EZH2
GO:0006954~inflammatory response	0.0022	SP100, TNFAIP6, IL2RA, CCL3L3, REL, TNFAIP3, IL19, CCR7, NFKB1

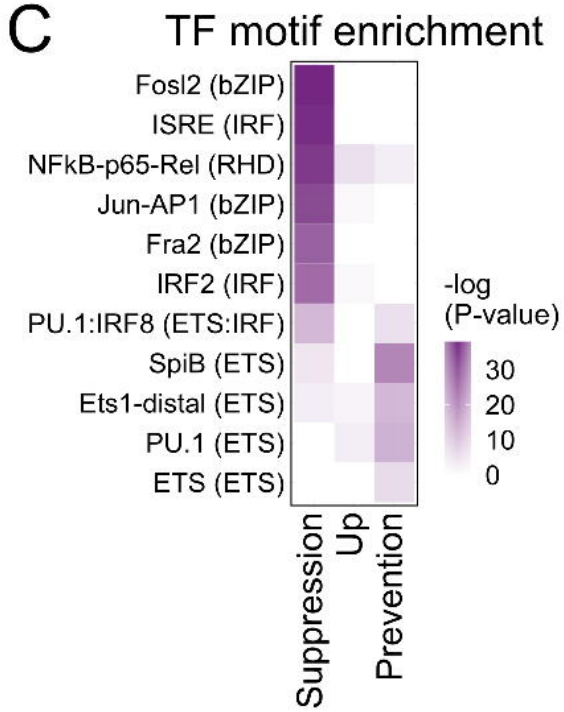

A

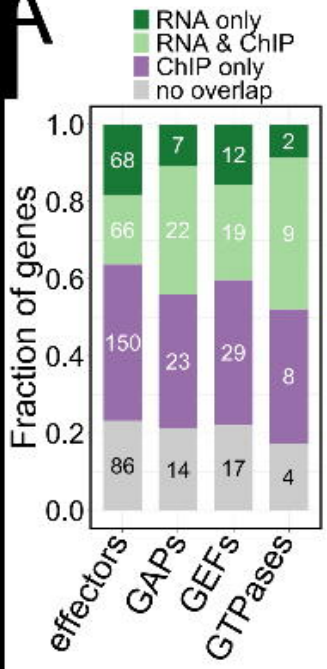

B

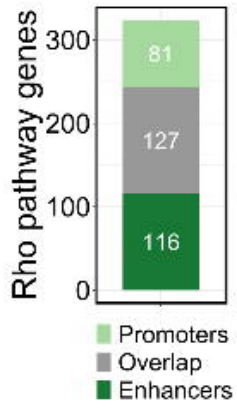

C

Rho GTPase pathway genes associated with enhancers

number of associated enhancers	number of genes	% total enhancer associated genes
1	85	35.0
2	46	18.9
3	36	14.8
4	20	8.2
5	14	5.8
6	12	4.9
7	13	5.3
8	5	2.1
9	3	1.2
10	3	1.2
11	2	0.8
12	1	0.4
13	2	0.8
14	1	0.4

D

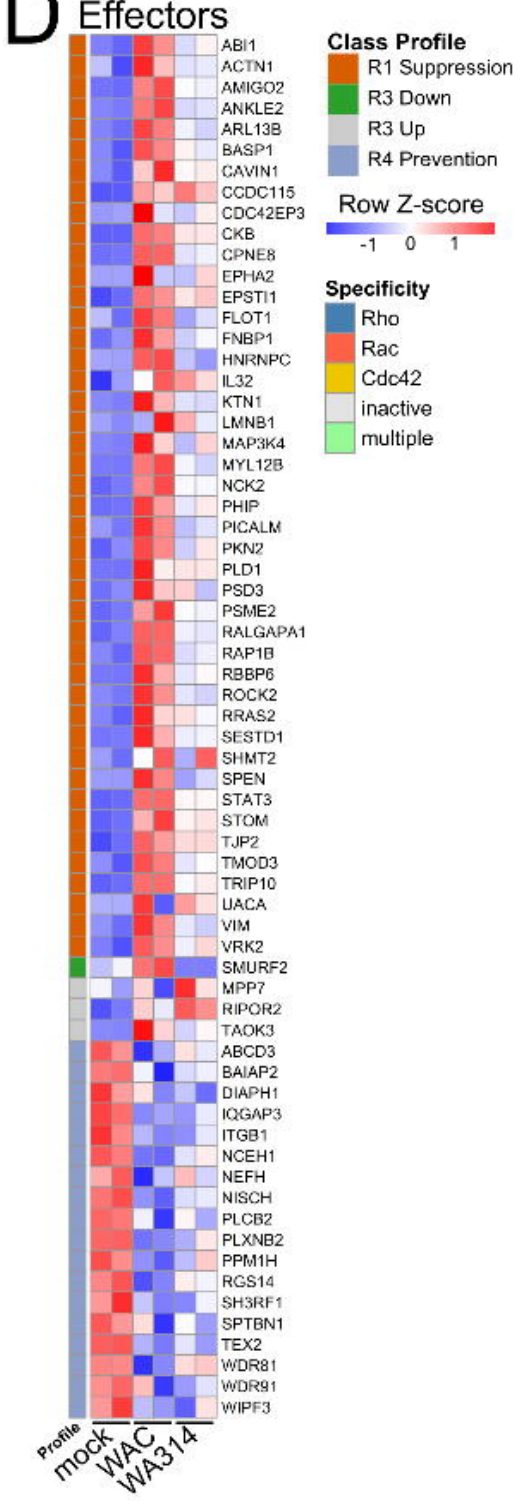

E

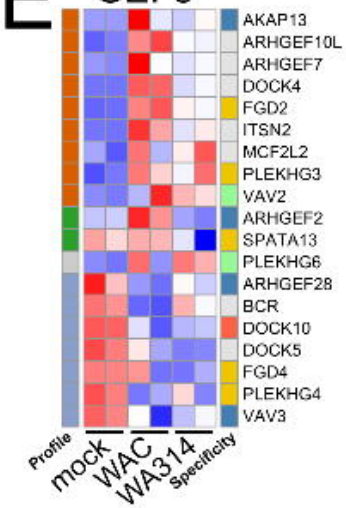

F

Rho GTPase effector specificity

	Prevention	Suppression	Up	Down
Cdc42	7	11	0	0
Rac1	6	10	2	1
RhoA	5	10	0	0
RhoB	2	8	1	0
Rac3	2	5	2	0
RhoC	2	7	0	0
Rac2	1	4	2	0
Rnd3	1	5	0	0
RhoBTB1	0	4	0	0
RhoBTB2	0	4	0	0
RhoF	0	5	0	0
RhoD	1	4	0	0
RhoG	1	4	1	0
RhoJ	1	4	1	0
RhoQ	1	4	1	0
RhoV	2	3	0	0
Rnd2	1	3	0	0
RhoH	0	4	0	0
Rnd1	0	3	0	0
RhoU	1	2	0	0
unique effectors	18	44	3	1

A

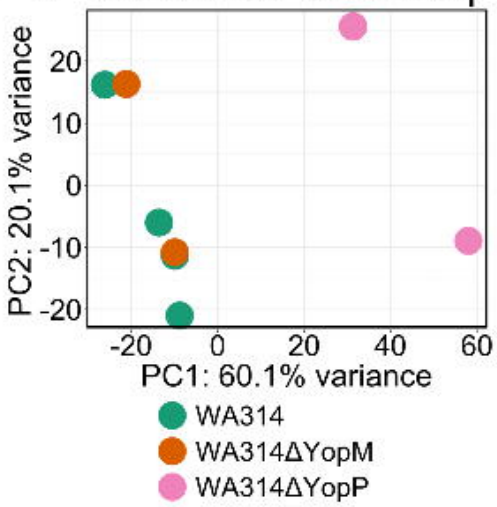

B

% YopP effect on histone modifications

Profile	Class	% YopP effect
Suppression	P1a	57.2
	P2a	43.4
	E1	48.6
Down	P2b	8.9
	E2	25.2
Up	P2c	25.9
	E3	28.3
Prevention	P1b	40.5
	P2d	52.0
	E4	53.2
	Median	**42.0**

C

% YopP effect on gene expression

Profile	Class	% YopP effect
Suppression	R1	46.9
Down	R2	26.4
Up	R3	65.7
Prevention	R4	55.8
	Median	**51.4**

D

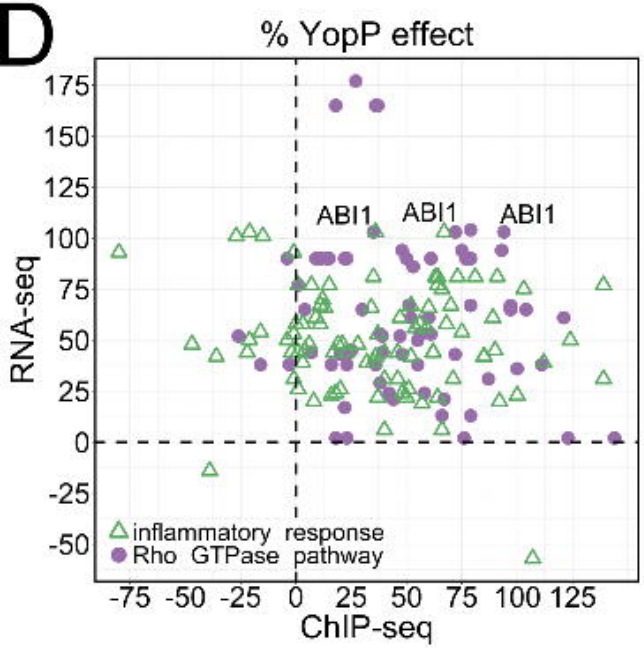

E